difference between normal lymphocyte differentiation and lymphoma cell phenotype polarization, our findings suggest that miRNAs might be widely involved in this reciprocal regulatory network between helper T-cell differentiation programs. The STAT3–miR-135b–GATA3/STAT6 connection revealed in this study might propose inhibitory mechanism(s) against Th2 in Th17 differentiation program, mirroring the opposite inhibitory impacts of Th1 and Th2 programs on Th17 differentiation,[24,26] for ensuring mutual exclusion.

In conclusion, our study demonstrates a novel oncogenic pathway composed of NPM-ALK, STAT3, and miR-135b that authorizes IL-17–producing immunophenotype of ALCL. Tumor suppression with miR-135b blockade also demonstrates the therapeutic potential of miR-135b interference strategy targeting the "Th17 mimic" axis. These findings might advance our understandings of ALK-mediated oncogenesis and be useful for the development of new therapeutic interventions.

Acknowledgments

The authors thank E. Johansson, Y. Morishita, K. Kiyono, M. Morikawa, Y. Yoshimatsu, K. Isogaya, and H. Mihira for discussion and skilled technical assistance and all members of the Department of Molecular Pathology, University of Tokyo.

This work was supported by KAKENHI (Grants-in-Aid for Scientific Research for Research Activity start-up 22890038 and Innovative Areas "RNA regulation" 23112702); the Global Center of Excellence Program for "Integrative Life Science Based on the Study of Biosignaling Mechanisms" from the Ministry of Education, Culture, Sports, Science and Technology of Japan; and the Cell Science Research Foundation.

Authorship

Contribution: H. Matsuyama and H.I.S. conceived and designed the research; H. Matsuyama performed experiments and analyses and wrote the paper; H.I.S. provided key materials and analyzed and wrote the paper; H.N. performed animal experiments and analysis; M.N., T.Y., N.K., H. Mano and K.S. provided clinical samples; and K.S. and K.M. supervised the whole project and wrote the paper.

Conflict-of-interest disclosure: The authors declare no competing financial interests.

Correspondence: Kohei Miyazono, Department of Molecular Pathology, Graduate School of Medicine, University of Tokyo, 7-3-1 Hongo, Bunkyo-ku, Tokyo 113-0033, Japan; e-mail: miyazono@m.u-tokyo.ac.jp.

References

1. Ambros V, Chen X. The regulation of genes and genomes by small RNAs. *Development.* 2007; 134(9):1635-1641.
2. O'Connell RM, Rao DS, Chaudhuri AA, Baltimore D. Physiological and pathological roles for microRNAs in the immune system. *Nat Rev Immunol.* 2010; 10(2):111-122.
3. Croce CM. Causes and consequences of microRNA dysregulation in cancer. *Nat Rev Genet.* 2009;10(10):704-714.
4. Staudt LM, Dave S. The biology of human lymphoid malignancies revealed by gene expression profiling. *Adv Immunol.* 2005;87:163-208.
5. Alizadeh AA, Eisen MB, Davis RE, et al. Distinct types of diffuse large B-cell lymphoma identified by gene expression profiling. *Nature.* 2000; 403(6769):503-511.
6. Suzuki HI, Miyazono K. Emerging complexity of microRNA generation cascades. *J Biochem.* 2011;149(1):15-25.
7. He L, Thomson JM, Hemann MT, et al. A microRNA polycistron as a potential human oncogene. *Nature.* 2005;435(7043):828-833.
8. Suzuki HI, Yamagata K, Sugimoto K, Iwamoto T, Kato S, Miyazono K. Modulation of microRNA processing by p53. *Nature.* 2009;460(7254):529-533.
9. Chiarle R, Voena C, Ambrogio C, Piva R, Inghirami G. The anaplastic lymphoma kinase in the pathogenesis of cancer. *Nat Rev Cancer.* 2008;8(1):11-23.
10. Soda M, Choi YL, Enomoto M, et al. Identification of the transforming EML4-ALK fusion gene in non-small-cell lung cancer. *Nature.* 2007; 448(7153):561-566.
11. Haraguchi T, Ozaki Y, Iba H. Vectors expressing efficient RNA decoys achieve the long-term suppression of specific microRNA activity in mammalian cells. *Nucleic Acids Res.* 2009;37(6):e43.
12. Piva R, Pellegrino E, Mattioli M, et al. Functional validation of the anaplastic lymphoma kinase signature identifies CEBPB and BCL2A1 as critical target genes. *J Clin Invest.* 2006;116(12):3171-3182.
13. Anastasov N, Klier M, Koch I, et al. Efficient shRNA delivery into B and T lymphoma cells using lentiviral vector-mediated transfer. *J Hematop.* 2009;2(1):9-19.
14. Bromberg JF, Wrzeszczynska MH, Devgan G, et al. Stat3 as an oncogene. *Cell.* 1999;98(3): 295-303.
15. Iqbal J, Weisenburger DD, Greiner TC, et al. Molecular signatures to improve diagnosis in peripheral T-cell lymphoma and prognostication in angioimmunoblastic T-cell lymphoma. *Blood.* 2010; 115(5):1026-1036.
16. Subramanian A, Tamayo P, Mootha VK, et al. Gene set enrichment analysis: a knowledge-based approach for interpreting genome-wide expression profiles. *Proc Natl Acad Sci U S A.* 2005;102(43):15545-15550.
17. Lawrie CH, Saunders NJ, Soneji S, et al. MicroRNA expression in lymphocyte development and malignancy. *Leukemia.* 2008;22(7): 1440-1446.
18. Saito T, Saetrom P. MicroRNAs–targeting and target prediction. *N Biotechnol.* 2010; 27(3):243-249.
19. Nagel R, le Sage C, Diosdado B, et al. Regulation of the adenomatous polyposis coli gene by the miR-135 family in colorectal cancer. *Cancer Res.* 2008;68(14):5795-5802.
20. Kuiper RP, Schoenmakers EF, van Reijmersdal SV, et al. High-resolution genomic profiling of childhood ALL reveals novel recurrent genetic lesions affecting pathways involved in lymphocyte differentiation and cell cycle progression. *Leukemia.* 2007;21(6):1258-1266.
21. Gu TL, Tothova Z, Scheijen B, Griffin JD, Gilliland DG, Sternberg DW. NPM-ALK fusion kinase of anaplastic large-cell lymphoma regulates survival and proliferative signaling through modulation of FOXO3a. *Blood.* 2004;103(12): 4622-4629.
22. Greer EL, Brunet A. FOXO transcription factors at the interface between longevity and tumor suppression. *Oncogene.* 2005;24(50):7410-7425.
23. Ambrogio C, Martinengo C, Voena C, et al. NPM-ALK oncogenic tyrosine kinase controls T-cell identity by transcriptional regulation and epigenetic silencing in lymphoma cells. *Cancer Res.* 2009;69(22):8611-8619.
24. Harrington LE, Hatton RD, Mangan PR, et al. Interleukin 17-producing CD4+ effector T cells develop via a lineage distinct from the T helper type 1 and 2 lineages. *Nat Immunol.* 2005;6(11):1123-1132.
25. Zhou M, Ouyang W. The function role of GATA-3 in Th1 and Th2 differentiation. *Immunol Res.* 2003;28(1):25-37.
26. McGeachy MJ, Cua DJ. Th17 cell differentiation: the long and winding road. *Immunity.* 2008;28(4): 445-453.
27. Lazarevic V, Chen X, Shim JH, et al. T-bet represses T(H)17 differentiation by preventing Runx1-mediated activation of the gene encoding RORgammat. *Nat Immunol.* 2011;12(1):96-104.
28. van Hamburg JP, Mus AM, de Bruijn MJ, et al. GATA-3 protects against severe joint inflammation and bone erosion and reduces differentiation of Th17 cells during experimental arthritis. *Arthritis Rheum.* 2009;60(3):750-759.
29. Okamoto K, Iwai Y, Oh-Hora M, et al. Ikappa-Bzeta regulates T(H)17 development by cooperating with ROR nuclear receptors. *Nature.* 2010; 464(7293):1381-1385.
30. Yang XO, Chang SH, Park H, et al. Regulation of inflammatory responses by IL-17F. *J Exp Med.* 2008;205(5):1063-1075.
31. Ji Y, Zhang W. Th17 cells: positive or negative role in tumor? *Cancer Immunol Immunother.* 2010;59(7):979-987.
32. Zou W, Restifo NP. T(H)17 cells in tumour immunity and immunotherapy. *Nat Rev Immunol.* 2010; 10(4):248-256.
33. Numasaki M, Fukushi J, Ono M, et al. Interleukin-17 promotes angiogenesis and tumor growth. *Blood.* 2003;101(7):2620-2627.
34. Numasaki M, Watanabe M, Suzuki T, et al. IL-17 enhances the net angiogenic activity and in vivo growth of human non-small cell lung cancer in SCID mice through promoting CXCR-2-dependent angiogenesis. *J Immunol.* 2005;175(9): 6177-6189.

35. Lin CH, Jackson AL, Guo J, Linsley PS, Eisenman RN. Myc-regulated microRNAs attenuate embryonic stem cell differentiation. *EMBO J.* 2009;28(20):3157-3170.
36. Tong AW, Fulgham P, Jay C, et al. MicroRNA profile analysis of human prostate cancers. *Cancer Gene Ther.* 2009;16(3):206-216.
37. Bowman T, Garcia R, Turkson J, Jove R. STATs in oncogenesis. *Oncogene.* 2000;19(21):2474-2488.
38. Yuki D, Lin YM, Fujii Y, Nakamura Y, Furukawa Y. Isolation of LEM domain-containing 1, a novel testis-specific gene expressed in colorectal cancers. *Oncol Rep.* 2004;12(2):275-280.
39. Jones AM, Douglas EJ, Halford SE, et al. Array-CGH analysis of microsatellite-stable, near-diploid bowel cancers and comparison with other types of colorectal carcinoma. *Oncogene.* 2005; 24(1):118-129.
40. Douglas EJ, Fiegler H, Rowan A, et al. Array comparative genomic hybridization analysis of colorectal cancer cell lines and primary carcinomas. *Cancer Res.* 2004;64(14):4817-4825.
41. Swerdlow SH, Campo E, Harris NL, et al. *WHO Classification of Tumours of Haematopoietic and Lymphoid Tissues.* 4th ed. Lyon, France: IARC; 2008.
42. Savan R, McFarland AP, Reynolds DA, et al. A novel role for IL-22R1 as a driver of inflammation. *Blood.* 2011;117(2):575-584.
43. Küppers R. The biology of Hodgkin's lymphoma. *Nat Rev Cancer.* 2009;9(1):15-27.
44. Tripodo C, Gri G, Piccaluga PP, et al. Mast cells and Th17 cells contribute to the lymphoma-associated pro-inflammatory microenvironment of angioimmunoblastic T-cell lymphoma. *Am J Pathol.* 2010;177(2):792-802.
45. Mann KP, Hall B, Kamino H, Borowitz MJ, Ratech H. Neutrophil-rich, Ki-1-positive anaplastic large-cell malignant lymphoma. *Am J Surg Pathol.* 1995;19(4):407-416.
46. Tamiolakis D, Georgiou G, Prassopoulos P, Simopoulos C, Venizelos J, Papadopoulos N. Neutrophil-rich anaplastic large cell lymphoma (NR-ALCL) mimicking lymphadenitis: a study by fine-needle aspiration biopsy. *Leuk Lymphoma.* 2004; 45(6):1309-1310.
47. Engsig FN, Moller MB, Hasselbalch HK, Mahdi B, Obel N. Extreme neutrophil granulocytosis in a patient with anaplastic large cell lymphoma of T-cell lineage. *APMIS.* 2007;115(6):778-783.
48. Suzuki HI, Miyazono K. Dynamics of microRNA biogenesis: crosstalk between p53 network and microRNA processing pathway. *J Mol Med.* 2010; 88(11):1085-1094.
49. Du C, Liu C, Kang J, et al. MicroRNA miR-326 regulates TH-17 differentiation and is associated with the pathogenesis of multiple sclerosis. *Nat Immunol.* 2009;10(12):1252-1259.
50. O'Connell RM, Kahn D, Gibson WS, et al. MicroRNA-155 promotes autoimmune inflammation by enhancing inflammatory T cell development. *Immunity.* 2010;33(4):607-619.

Dicer Plays Essential Roles for Retinal Development by Regulation of Survival and Differentiation

Atsumi Iida,[1,2] *Toru Shinoe,*[1,2] *Yukihiro Baba,*[1] *Hiroyuki Mano,*[3] *and Sumiko Watanabe*[1]

Purpose. Much attention has been paid to the roles of microRNA in developmental and biological processes. Dicer plays essential roles in cell survival and proliferation in various organs. We examined the role of Dicer in retinal development using retina-specific conditional knockout of Dicer in mice.

Methods. Dkk3-Cre expressed the *Cre* gene in retinal progenitor cells from an early embryonic stage. The authors analyzed Dkk-Cre/Dicer-flox (Dicer-CKO) mice for their survival, proliferation, and differentiation. To analyze the role of Dicer in later stages of retinal development, a Cre expression plasmid was introduced into the neonatal retina by electroporation, and retinal differentiation was examined.

Results. Dicer-CKO mice were born at the numbers we expected, based on Mendelian genetics, but their eyes never opened. Massive death of retinal progenitor cells occurred during embryogenesis, resulting in microphthalmia, and most retinal cells had disappeared by postnatal day 14. In vitro reaggregation culture of Dicer-CKO retinal cells showed that cell death and the suppression of proliferation by Dicer inactivation occurred in a cell-autonomous manner. Cell differentiation markers were expressed in the Dicer-CKO retina; however, these cells localized abnormally, and the inner plexiform layer was absent, suggesting that cell migration and morphologic differentiation, especially process extension, were perturbed. Forced neonatal expression of Cre induced apoptosis and affected the expression of differentiation markers.

Conclusions. Taken together, these results show that Dicer is essential during early retinal development. (*Invest Ophthalmol Vis Sci.* 2011;52:3008-3017) DOI:10.1167/iovs.10-6428

The vertebrate neural retina is organized into a laminar structure comprising six types of neuron and glial cell, including Müller glia and microglia. During retinogenesis, these various cell types are derived from a common population of multipotent retinal progenitor cells in a relatively fixed chronological sequence.[1] Intrinsic cues and extrinsic signals play critical roles in defining the types of cells generated from common retinal progenitor cells,[2,3] and various molecules are involved in this process. The expression of these genes in retinal development is regulated at various levels; microRNA (miRNA) is one such regulator.

MicroRNAs are small, noncoding RNAs that are encoded in the genomes of all metazoans. They are essential in the proliferation and differentiation of various tissues, including stem cells.[4-6] The roles of miRNAs in retina have been reported,[7,8] and a recent study showed the presence of light-regulated retinal miRNAs.[9] In addition to suppressing the function of certain miRNAs, we can remove all miRNAs by deleting enzymes that are essential in their biosynthesis. DGCR8 is required for the production of all canonical miRNAs, and Dicer is an enzyme that cleaves double-stranded RNA into miRNA.[10] The removal of DGCR8 or Dicer results in a defective cell cycle and silencing of the self-renewal program of embryonic stem cells.[11,12] Because the complete loss of Dicer in mice results in early embryonic death,[13] mice with a conditional allele of the Dicer gene have been produced,[14] enabling the study of the roles of miRNA in organogenesis. Subsequently, essential roles of Dicer in organogenesis have been revealed by studying mice with various tissue-specific expression of Cre.[14,15]

In neurons, the deletion of Dicer by α-calmodulin kinase II Cre results in an array of phenotypes, including microcephaly and reduced dendritic branch elaboration, suggesting that the loss of Dicer disrupts cellular and tissue morphogenesis in the cortex and hippocampus.[16] The first study examining the roles of Dicer in the retina using Chx10-Cre transgenes, expected to express Cre in retinal progenitor cells, showed that although Chx10 was expressed in the embryonic retina, morphologic defects were observed at postnatal day (P) 16 with the formation of photoreceptor rosettes, accompanied by abnormal electroretinogram responses.[17] However, the relatively mild phenotype of the mice is surmised to be caused by mosaic expression of Cre in the Chx10-Cre transgenic retina[17] because subsequent work by George and Reh using αPax6-Cre-retina specific Dicer conditional knockout showed that Dicer is required in retinal development.[18] In this work, we evaluated the effects of deleting Dicer using Dkk3-Cre mice, which expressed the *Cre* gene in retinal progenitor cells from an early embryonic stage.[19]

Materials and Methods

Mice and Reagents

EGFP transgenic mice, which express the *EGFP* gene ubiquitously through the CAG promoter, were kindly provided by Masaru Okabe (Osaka University).[20,21] $Dicer^{flox}$ mice[14] were kindly provided by Michael McManus (University of California, San Francisco), and Dkk3-Cre BAC transgenic mice were as previously described.[19] $Dicer^{flox/flox}$ (Dicer-fl/fl) or $Dicer^{flox/wild}$ were used as controls for experiments shown in Figures 1 and 2. ICR mice were obtained from Japan SLC Co. All animal experiments were approved by the Animal Care Committee of the Institute of Medical Science, University of Tokyo, and were conducted in accordance with the ARVO Statement for the Use of Animals in Ophthalmic and Vision Research.

From the [1]Division of Molecular and Developmental Biology, Institute of Medical Science, University of Tokyo, Tokyo, Japan; and the [3]Division of Functional Genomics, Jichi Medical University, Tochigi, Japan.

[2]These authors contributed equally to the work presented here and should therefore be regarded as equivalent authors.

Supported by MEXT, Japan.

Submitted for publication August 18, 2010; revised October 18 and December 7 and 14, 2010; accepted December 15, 2010.

Disclosure: **A. Iida**, None; **T. Shinoe**, None; **Y. Baba**, None; **H. Mano**, None; **S. Watanabe**, None

Corresponding author: Sumiko Watanabe, Division of Molecular and Developmental Biology, Institute of Medical Science, University of Tokyo, 4-6-1 Shirokanedai, Minato-ku, Tokyo 108-8639, Japan; sumiko@ims.u-tokyo.ac.jp.

Investigative Ophthalmology & Visual Science, May 2011, Vol. 52, No. 6

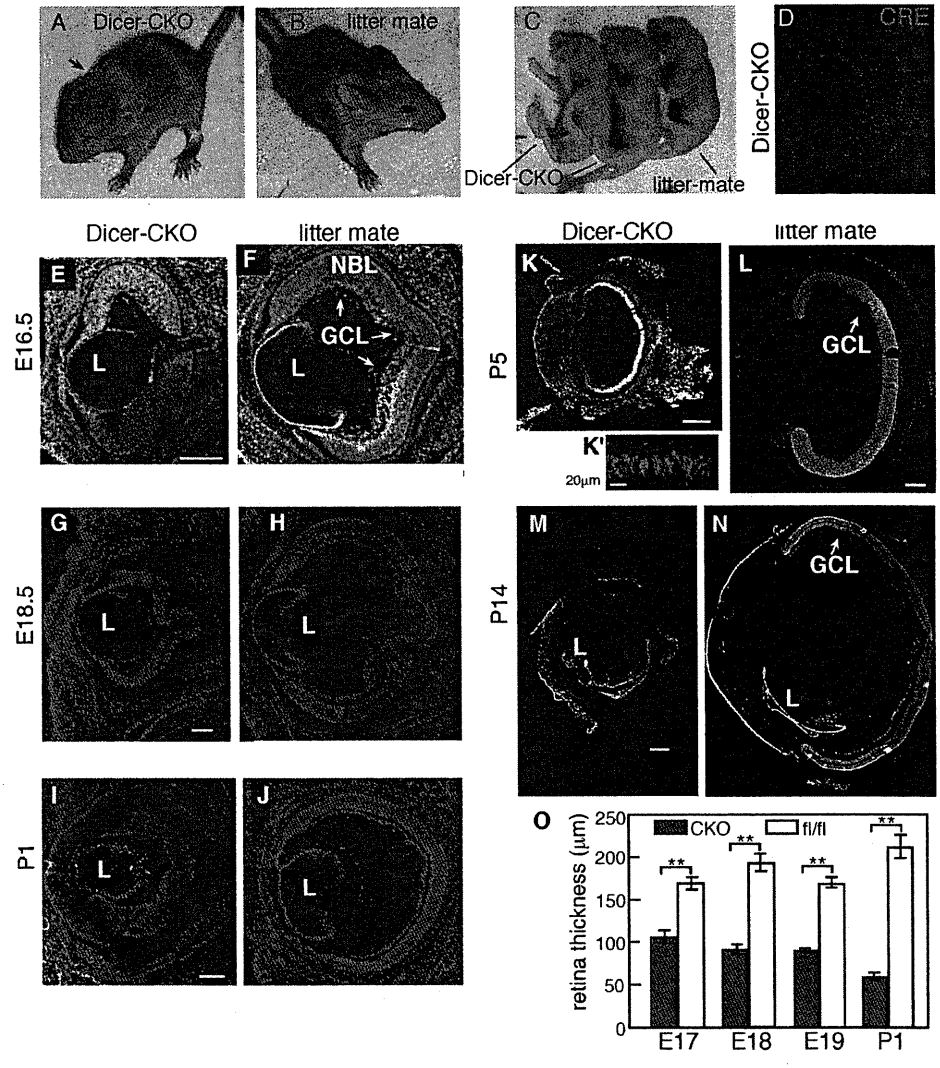

FIGURE 1. Dicer$^{lox/lox}$:Dkk3$^{+/cre}$ (Dicer-CKO) mice were born but had microphthalmia. (**A–C**) Images of Dicer-CKO (**A**) and littermate (**B**) mice at 2 weeks of age. Images of embryos of Dicer-CKO and littermate at E16.5 (**C**). (**D**) Immunostaining of Cre expression of Dicer-CKO retina at E17.5 was performed using frozen sections. (**E–N**) Structure of the eye of Dicer-CKO and littermate at E16.5 (**E**, **F**), E18.5 (**G**, **H**), P1 (**I**, **J**), P5 (**K**, **L**), and P14 (**M**, **N**) stages. Head (**E–J**) or whole eyes (**K–N**) were frozen sectioned, and nuclei were visualized by staining of DAPI. L, lens. Scale bar, 200 μm unless indicated. L, lens; NBL, neuroblastic layer. (**O**) Thickness of retina of Dicer-CKO or fl/fl control mice. Measurements were made under a microscope, and the thickness of retina at central region was examined at indicated stages. Average of three independent retinas with SD is shown. $^{**}P < 0.01$, Student's *t*-test.

DNA Construction

pxCANCre containing CAG promoter followed by *Cre* genes was the gift of Izumu Saito (University of Tokyo). CAG-Cre-IRES-EGFP was constructed by the ligation of fragments of CAG-Cre (*SalI-BglII*), IRES-EGFP (*BglII-NotI*), and the vector portion from pEGFP2 (*SalI-NotI*).

Immunostaining

Immunostaining of sectioned or dissociated retina was performed as described previously.[22] OCT compound (Tissue-Tek)–embedded samples were sectioned with 10-μm thickness by a cryostat (CM3050S; Leica, Wetzlar, Germany). Primary antibodies used were the following: mouse monoclonal antibodies against βIII tubulin (Covance, Princeton, NJ), photoreceptor-specific nuclear receptor ([PNR], ppmx), rhodopsin (Rho4D2, kindly donated by Robert S. Molday, University of British Columbia), glutamine synthetase (GS; Chemicon, Temecula, CA), HuC/D (Molecular Probes, Eugene, OR), Ki67 (BD Biosciences, Franklin Lakes, NJ), Cre (Millipore, Billerica, MA), rabbit polyclonal antibody against GFP (Clontech, Palo Alto, CA), Pax6 (Covance), calbindin (Millipore), active-caspase3 (Promega, Madison, WI), and goat polyclonal antibody anti-Brn3b (Santa Cruz Biotechnology, Santa Cruz, CA). All antibodies against retinal subtypes have been used by us and confirmed to recognize mouse retina.[23–25] The first antibodies were visualized by using appropriate Alexa 488 or Alexa 546-conjugated secondary antibodies (Molecular Probes). Samples were mounted in reagent (VectaShield; Vector Laboratories, Burlingame, CA) and analyzed under a microscope (Axioplan; Zeiss, Oberkochen, Germany).

Retinal Cultures and Electroporation

Reaggregation cultures were set up as described earlier.[23] Briefly, retinal cells of Dicer-CKO:GFP or GFP mice at embryonic day (E) 16 were dissociated and mixed with far larger numbers of host retinal cells isolated from normal ICR mice at E16. The ratio of donor to host cells was 5:95. Electroporation was performed using an electroporator (CUY21; Nepa Gene, Chiba, Japan) and electrode (CYU520P5; Nepa Gene), as described.[26] Briefly, retinas were transferred to a microelectroporation chamber filled with plasmid solution (1 mg/mL in Hanks' balanced salt solution), and four square pulses (25 V) of 50-μs duration with 950-μs intervals were applied using a pulse generator (CUY21; Nepa Gene).

RESULTS

Inactivation of Dicer in Retinal Progenitor Cells Results in Severe Retinal Malformation

To inactivate Dicer in retinal progenitor cells, we used Dkk3-Cre mice, which express Cre recombinase beginning on at least E10.5 in a retina-specific manner.[19] The expected num-

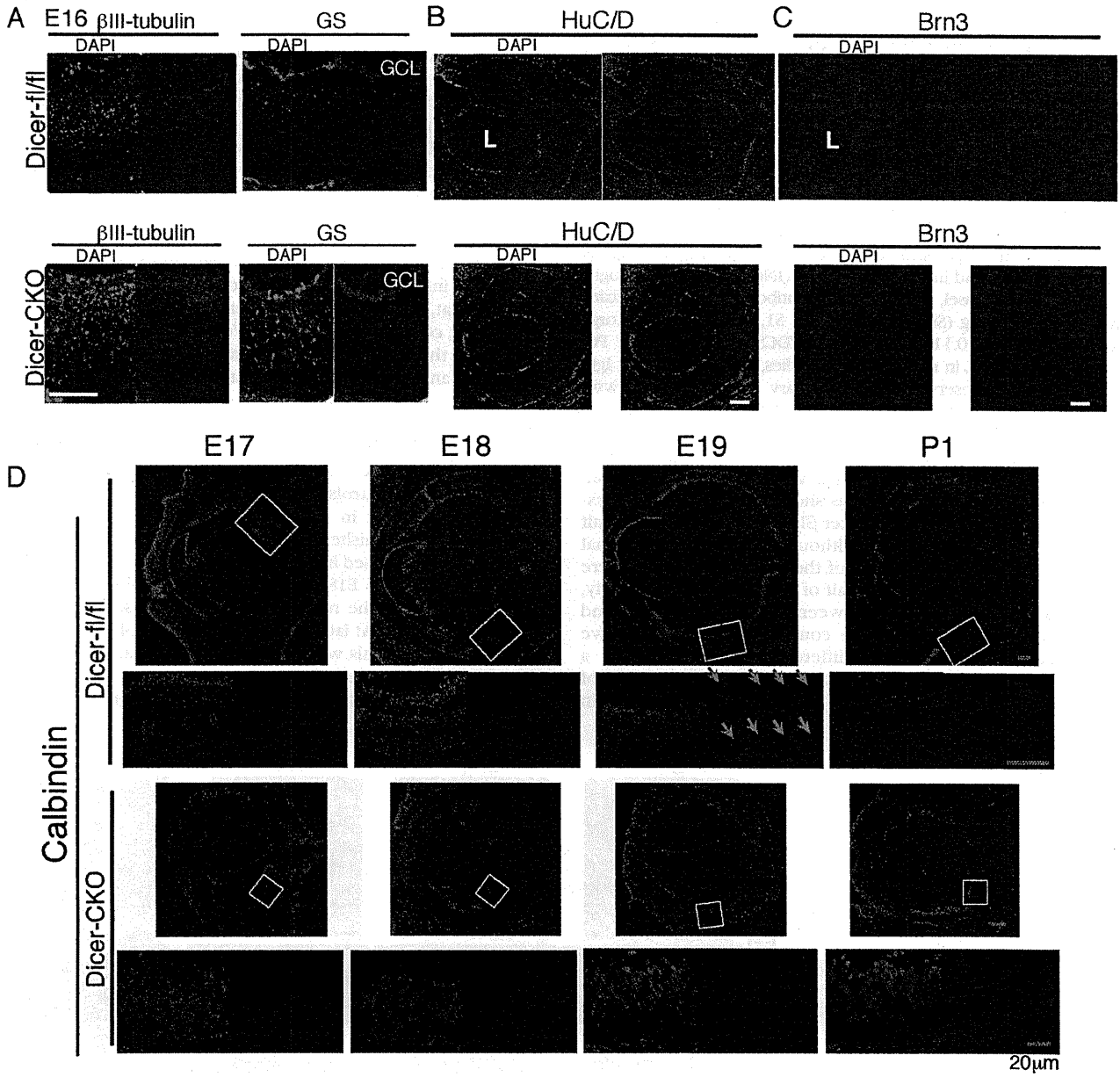

FIGURE 2. Detailed examination of retinal development by immunostaining of retinas of Dicer-CKO mice revealed perturbation of retinal development. (**A–D**) Retinas from Dicer-CKO or littermate control mice at E16 (**A–C**) or indicated stages (**D**) were frozen sectioned. Immunostaining using indicated antibodies was performed, and nuclei were visualized by staining of DAPI. (**D**) *Lower* panels are enlarged images of the *white squared regions* in the *upper* panels. L, lens. Scale bars: 100 μm (**A**, **D**); 200 μm (**B**, **C**).

bers of $Dicer^{flox/flox}/Dkk3^{cre/-}$ (Dicer-CKO) mice, based on Mendelian genetics, were born, but they died approximately 4 to 6 weeks after birth for unknown reasons. Their eyes never opened (Fig. 1A), and they had small earlobes (Fig. 1A, red arrows), probably because of undetectable expression of Dkk3 in this region. The Dicer-CKO embryos were indistinguishable from their littermates in their appearance, except for their small eyes (Fig. 1C). During development, we examined eye structure in more detail using frozen sections. We first confirmed that Cre was expressed in nearly the whole area of the retina at E17.5 (Fig. 1D), as expected from the expression pattern of Dkk3-Cre original mice.[19] At E16.5, the retinas of the Dicer-CKO mice were already smaller than those of control mice (Figs. 1E, 1F). At this stage, the ganglion cell layer (GCL) was visible in control (Fig. 1E, arrows) but not in the Dicer-CKO (Fig. 1E) mice. At E18.5, the difference between retinal sphere diameters in the Dicer-CKO and littermates became clearer (Figs. 1G, 1H). At P1, the GCL and the inner plexiform layer (IPL) were clearly formed in the control retinas (Fig. 1J) but had not formed in the Dicer-CKO retinas. Retinal diameters were even smaller than those at E16.5 in Dicer-CKO mice, and the cells were not tightly linked (Fig. 1I). At P5, the retina was very thin, and no layered structure was observed in the Dicer-CKO mice (Fig. 1K'). At P14, the retina had no visible structure in Dicer-CKO mice, and there only a few cell aggregates remained in the central region in Dicer-CKO retinas (Fig. 1M).

We measured retinal thickness. Retinas of Dicer-CKO were thinner than those of control mice at E17 and constantly became thinner as development proceeded (Fig. 1O).

Differentiation Markers of Retinal Subtypes Were Once Expressed, Then Disappeared, as Retinal Development Proceeded

To examine the differentiation of retinal subtypes in the Dicer-CKO retina, we immunostained various markers of retinal subtypes using frozen sections. At first, control staining to examine nonspecific signal was performed using frozen, sectioned retinas at E17 and P6. Control immunoglobulin was used as the first antibody, and appropriate second antibodies conjugated with either Alexa 488 or Alexa 594 were stained. With E17 samples, mouse IgG showed nonspecific staining in regions around the GCL and inner nuclear layer (INL), which was thought to be the blood vessel, and rat primary antibody gave no significant nonspecific staining (Supplementary Fig. S1, http://www.iovs.org/lookup/suppl/doi:10.1167/iovs.10-6428/-/DCSupplemental). At P6, signals around GCL in mouse IgG antibodies, but not in the rat IgG antibody, were observed (Supplementary Fig. S1, http://www.iovs.org/lookup/suppl/doi:10.1167/iovs.10-6428/-/DCSupplemental). At E16, although the control retina had no layer structure except for the GCL, the inner half of the cells had became postmitotic whereas the outer half was still composed of undifferentiated progenitor cells, as shown by the restricted expression of the early neural marker βIII-tubulin in the inner half (Fig. 2A). In Dicer-CKO mice, although the βIII-tubulin signal was observed in the inner side of the Dicer-CKO retina, there were also signals in the outer half of the retina; consequently, there was no clear boundary between βIII-tubulin–positive and -negative fields, as seen in the controls (Fig. 2A). Then we examined the expression of differentiation markers. GS, a marker of Müller glia cells, was expressed in the inner half of the retina in controls (Fig. 2A). Again, like the βIII-tubulin staining pattern, GS expression was scattered throughout the Dicer-CKO retina, and no boundary between GS-positive and -negative regions was observed. HuC/D, a marker for amacrine and ganglion cells, and Brn3b, which is expressed in ganglion cells, were expressed in the innermost part of the control retina, forming a layer-like structure (Fig. 2B). In the Dicer-CKO retina, HuC/D was weakly expressed with relatively stronger intensity in the inner half of the retina (Fig. 2B). The Brn3b pattern was also expressed in the inner side, and strong signals were also observed in the outer region (Fig. 2C). Although Brn3-positive cells were seen in the innermost side of the retina, the IPL was not observed, suggesting that process extension is inhibited by the depletion of Dicer. These results indicate that, in Dicer-CKO mice, early differentiation of retinal progenitor cells was under way. We next examined the time course of the expression of several markers. Expression of calbindin, an amacrine and horizontal cell marker, was clearly observed as making lines in the outer region and GCL at E19 in controls (Fig. 2D, blue arrows). In the Dicer-CKO retina, expression of calbindin was observed, but positive cells did not make lines and were scattered in the whole area of the retina (Fig. 2D). At P1, controls showed an expression pattern similar to that at E19, but in Dicer-CKO retina, the expression of calbindin was diminished (Fig. 2D).

Brn3 was expressed in GCL at all examined stages in control retinas. At E17 and E18, Brn3 signals were observed at the innermost side of the retina, and it was also scattered at all areas of the retina. At later stages, the number of positive cells decreased, but signals were observed in all areas of the retina (Fig. 3A). We counted the Brn3-positive cells semiquantitatively, and the cell numbers of Brn3 were slightly fewer in

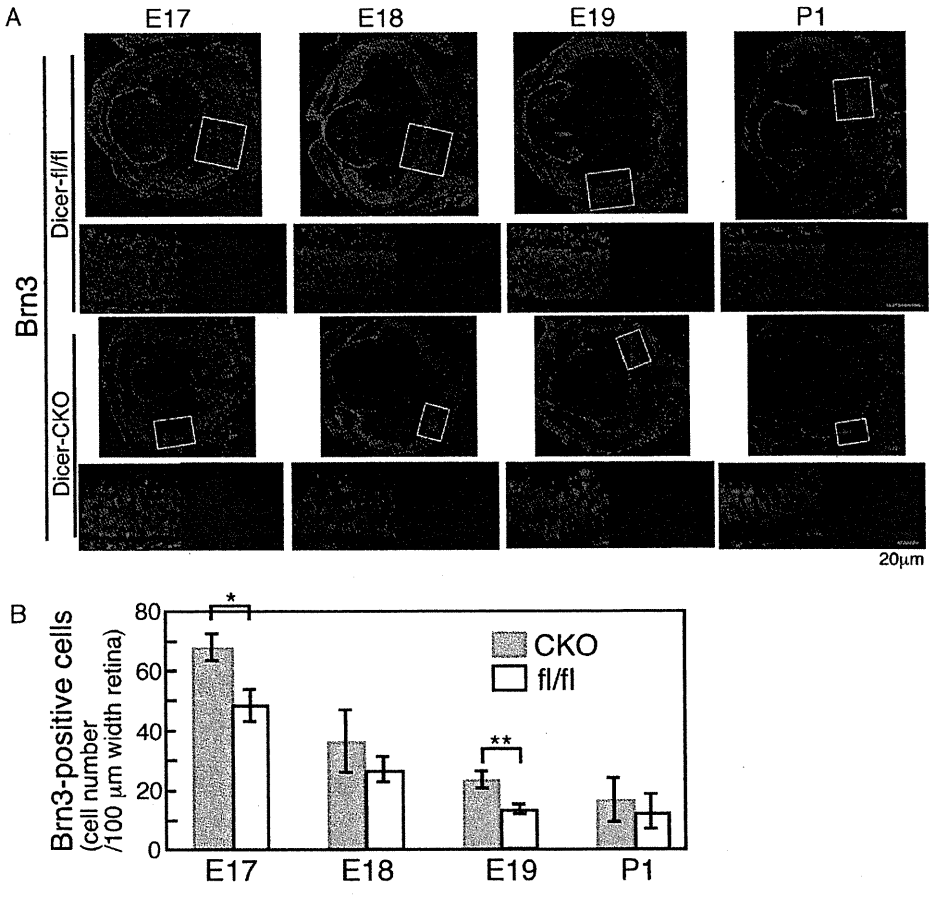

FIGURE 3. Enhanced expression of Brn3 in developing retinas of Dicer-CKO mice. (**A**) Retinas from Dicer-CKO or littermate control mice at indicated stages were frozen sectioned. Immunostaining using anti-Brn3 antibody was performed, and nuclei were visualized by DAPI staining. Scale bars, 100 μm. *Lower* panels are enlarged images of the *white squared regions* in the *upper* panels. (**B**) The number of Brn3-positive cells in the retina at indicated stages was examined. Brn3-positive cells at the central region of the retina were counted under a microscope in an area 100-μm wide. The average of three independent retinas with SD is shown. $^{**}P < 0.01$ and $^{*}P < 0.05$, were calculated by Student's *t*-test.

control than in Dicer-CKO (Fig. 3B) mice. Because the Dicer-CKO retina was thinner than the control retina (data not shown), the percentage of Brn3-positive cells in total retinal cells was much larger in Dicer-CKO than in control. At the P1 stage, Pax6 and PKC were weakly expressed in the whole retinal area (Fig. 4A). GS was not expressed in either control or Dicer-CKO retina, and some PNR-positive cells were observed in the Dicer-CKO retina although no signal was observed in the control retina (Figs. 4A, 4B). At P5, Hu, calbindin, and Pax6 signals were making lines near IPL in the control retina (Fig. 4B). However, in Dicer-CKO, no layer structure was observed even at this stage, but Hu, calbindin, Pax6, and Brn3B expression was observed in the whole retinal area (Fig. 4B).

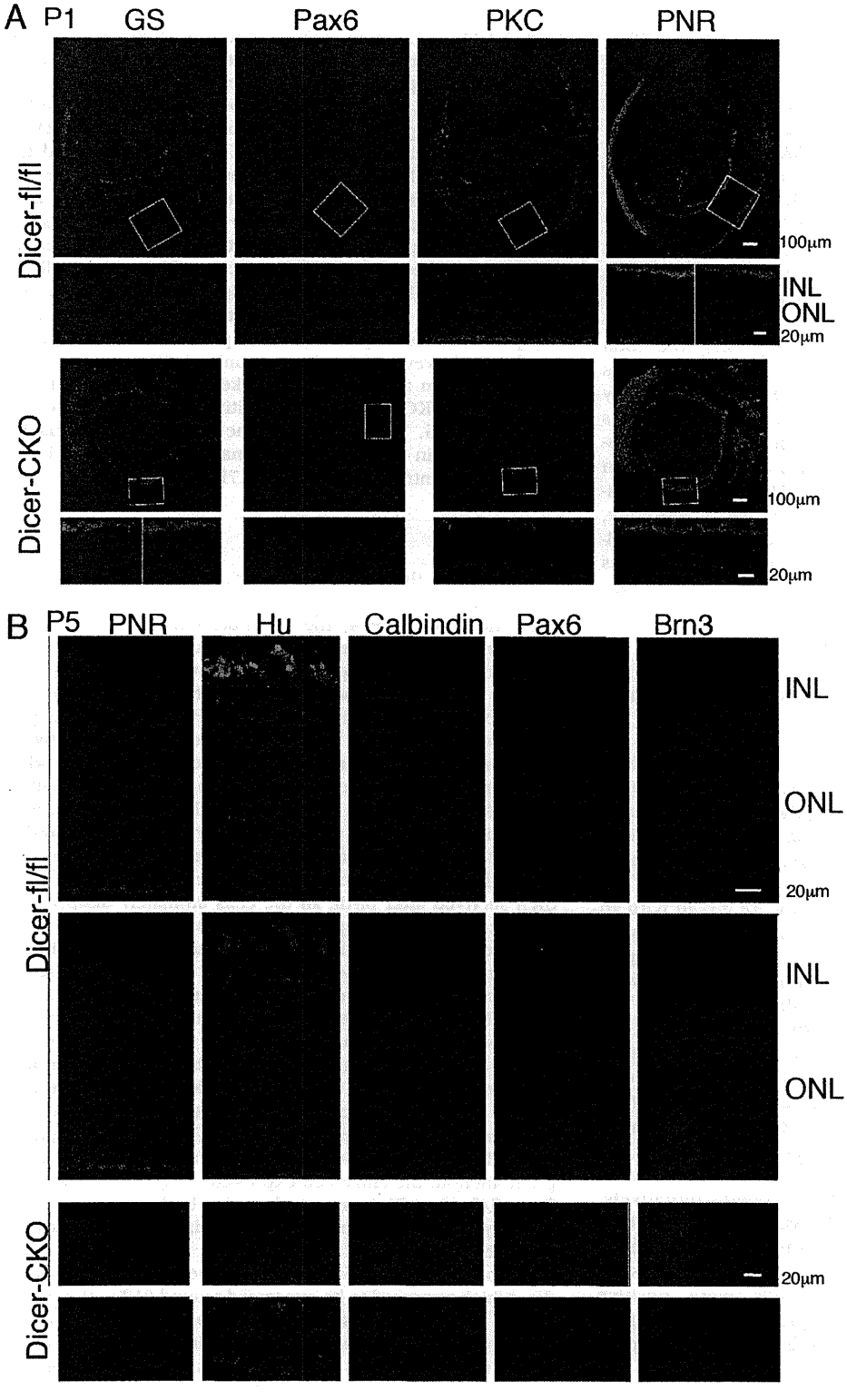

FIGURE 4. Disturbed expression of retinal marker proteins of Dicer-CKO mice after birth. (**A**, **B**) Retinas from dicer-CKO or littermate control mice at P1 (**A**) or P5 (**B**) were frozen sectioned. Immunostaining using indicated antibodies was performed, and nuclei were visualized by staining of DAPI. (**A**) *Lower* panels are enlarged images of the *white squared regions* in the *upper* panels. (**B**) DAPI-stained images. Scale bars are as indicated.

Next, we analyzed cell proliferation by examining anti-phospho-Histone H3, which is a marker of cells at the M phase of the cell cycle. As expected, signals were observed in the most apical edge in both control and Dicer-CKO retinas at E17 (Figs. 5A, 5B). In control samples at E18 and E19, patterns of staining were similar to those at E17 (Fig. 5A). In Dicer-CKO retina, positive signals were observed at the apical-most side, but in some regions, signals were also observed throughout the retinal region (Fig. 5B), suggesting that the layer structure was perturbed in the Dicer-CKO retina. In the P1 control retina, signals had disappeared from some portions of the central region but remained at the periphery (Fig. 5A, P1, inset). In the Dicer-CKO retina, strong signals were still observed in the central region. At P5, signals had completely disappeared from the central region (Fig. 5A, P5, upper panel) but remained in the peripheral region (Fig. 5A, P5, lower panel). In contrast, signals were still observed in both central and peripheral regions in the Dicer-CKO retina (Fig. 5B, P5). Semiquantitative counting of positive cells showed that until P19, the total number of phospho-Histone H3–positive cells was comparable between control and Dicer-CKO retinas (Fig. 5E). At P5, although no signal was observed in the central region of the control retina (Fig. 5A), the total number of phospho-Histone H3 in the control retina was larger than in the Dicer-CKO retina (Fig. 5E), probably because of the small size of the Dicer-CKO retina; this is supported by the finding that the population (%) of phospho-Histone H3–positive cells was bigger in Dicer-CKO than in controls in all examined stages (Fig. 5F). Then we examined cell apoptosis using anti-active caspase3 antibody, which was rarely expressed in any of the examined developmental stages in controls (Fig. 5C, E17~P5) but was strongly expressed in Dicer-CKO retinas at all stages (Fig. 5D, E17~P5), suggesting that abnormal apoptosis was induced in the Dicer-CKO retinas.

Apoptosis Induced by the Deletion of Dicer Is an Autonomous Cell Phenomenon

We examined whether the apoptosis observed in the Dicer-CKO retina was cell autonomous using reaggregation cultures, which are a good model for evaluating the intrinsic characteristics of proliferation and differentiation of donor cells in a defined environment.[23,27] To prepare reaggregation cultures, dissociated retinal cells from Dicer$^{flox/flox}$:GFP $^{+/GFP}$:Dkk3$^{+/cre}$ (Dicer-CKO/GFP) or GFP mice at E16.5 were mixed with an excess number of dissociated host retinal cells from wild-type mice at E16.5. After 5 or 8 days of culture, samples were harvested, frozen-sectioned, and immunostained with anti-GFP antibody. We found that although we used the same number of GFP-positive control or Dicer-CKO/GFP-derived cells in the aggregate cultures, the Dicer-CKO/GFP cells, but not the control GFP cells, decreased quickly during culture. After 8 days of culture, there were fewer than 50 Dicer-CKO cells but a large number of GFP-positive control cells (Fig. 6A). To quantify the results after culturing, we dissociated reaggregations, immunostained the dissociated cells, and counted immunopositive cells semiquantitatively. It was revealed that approximately 25% of Dicer-CKO/GFP cells were active caspase3-positive after 5 and 8 days of culture, whereas fewer than 2% (5 days) or 0% (8 days) of control GFP-positive or -negative cells were positive (Fig. 6B). We also examined the expression of rhodopsin and Pax6; no significant difference in expressing cell populations was observed (Figs. 6C, 6D).

Forced Expression of Cre around Birth Induced Apoptosis and Affected the Expression of Differentiation Markers

To examine the effect of deleting Dicer at a later stage of retinal development, the *Cre* gene was introduced into retinas isolated from Dicer-fl/fl or control mice at P1 using in vitro electroporation. First, we examined the expression of Cre protein by immunostaining frozen sections after 12 days of culture. Strong anti-Cre signals were observed, and most of the signals overlapped GFP signals (Fig. 7A). Apoptosis was also induced by Cre expression in the Dicer-fl/fl retina, but only a very small number of apoptotic cells appeared in the control retina (Fig. 7B). However, we cannot rule out the possibility that the electroporation procedure has a stronger apoptotic effect on Dicer-CKO retinas than on controls. Then we examined the expression of PNR and GS by immunostaining because rod photoreceptors and Müller glia differentiate at a relatively later stage of retinal development. Nearly 90% of the GFP-positive cells were PNR-positive in both control and Dicer-fl/fl retinas (Figs. 7C-E). There were slightly fewer GS-positive cells in control than in Dicer-fl/fl retinas (Figs. 7F, 7I). These results suggest that the differentiation of retinal cells into rod photoreceptors and Müller glia may not be perturbed by the deletion of Dicer. However, when we examined PKC (bipolar) and Islet1 (ganglion and amacrine) markers, we were not able to observe any PKC/EGFP double-positive cells in the Dicer-fl/fl retina (Fig. 7G, 7J). In addition, the number of islet1/EGFP-positive cells in the Dicer/fl/fl retina was significantly lower than in the control retina (Fig. 7H, 7K).

Discussion

We found that the deletion of Dicer in retinal progenitor cells during early development resulted in severe malformation of the retina; before P14, the Dicer-deleted retina had totally degenerated. In the Dicer-CKO retina, caspase was activated at all the examined developmental stages, suggesting that apoptosis was induced by the expression of Cre. Our finding is consistent with a previous study of αPax6-enhancer–dependent Dicer-CKO retinas,[18] reporting increased apoptosis by the deletion of Dicer in retinal progenitor cells. In addition, when we expressed Cre at a later stage (P1), the active caspase signal was observed to be at a significantly higher level than control, suggesting that Dicer is also essential for the survival of retinal cells after birth. This notion is supported by the finding that although some cells expressed differentiation markers and then survived after birth, all the cells ultimately disappeared, and the retina had completely degenerated before P14.

In contrast, retinal differentiation was less affected by the deletion of Dicer. Although localization was perturbed, retinal subtype marker–positive cells were present in the Dicer-CKO retina. In addition, in terms of marker expression, the forced expression of Cre in the later phase of development by electroporation supported the concept of the nonessential role of Dicer in differentiation. However, the detailed examination of marker expression patterns revealed that the effects of deletion of Dicer for each marker are different. The most striking is the upregulation of Brn3. Georgi and Reh[18] also observed a similar phenomenon: the enhanced expression of Brn3 in αPax6-Cre/Dicer-fl/fl mice. They report observing both the upregulation of early neuronal types (such as horizontal cells) and the downregulation of late progenitor cell markers.[18] We examined horizontal cell differentiation by the expression of calbindin, which appeared to be expressed around E19 in the control retina. We did not observe either ectopic expression before E19 or enhanced expression of calbindin in Dicer-CKO retina. In our mice, there was a possibility that the delayed onset of

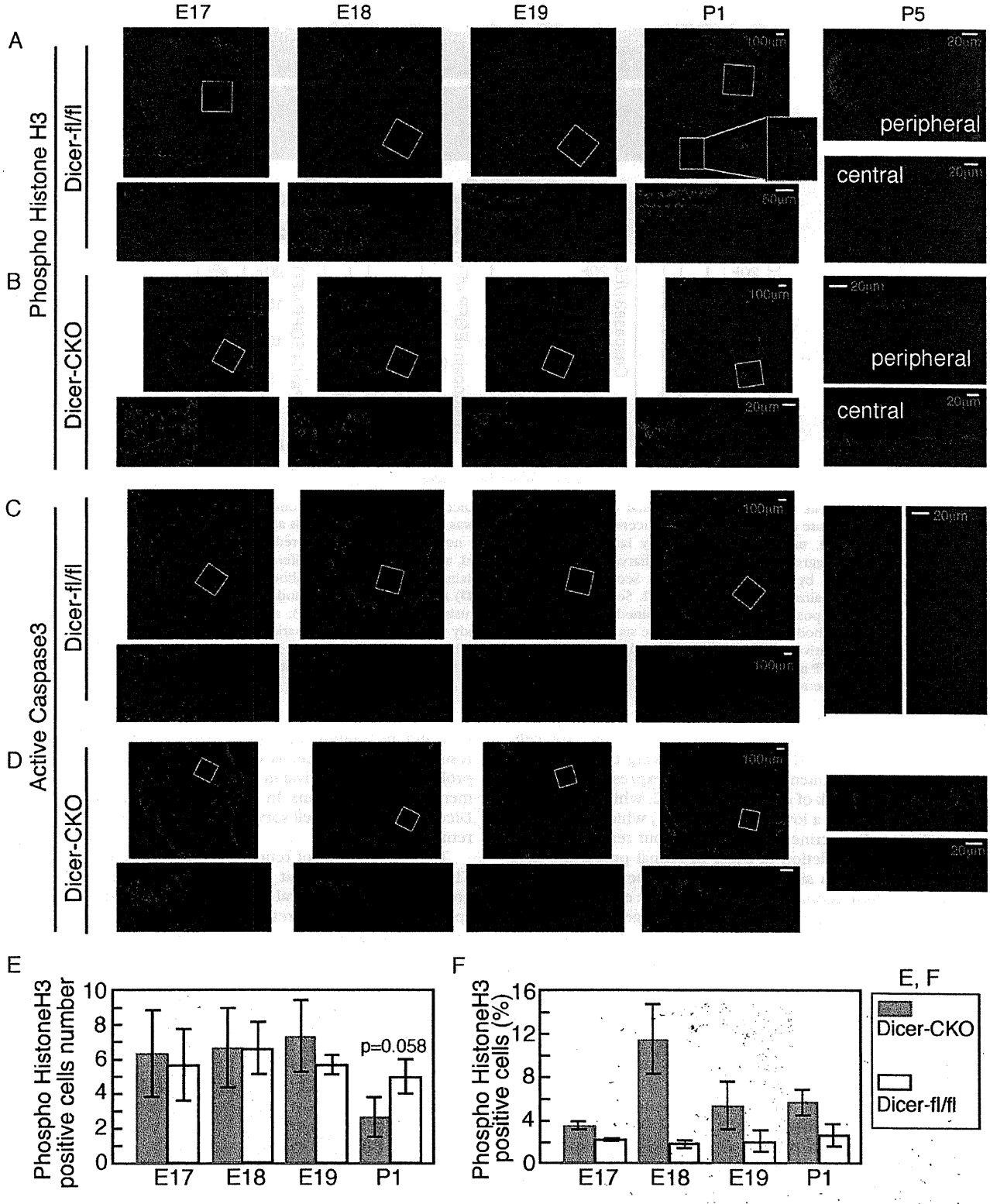

FIGURE 5. Proliferation was slightly suppressed, but massive cell death occurred in Dicer-CKO retinas. Retinas of Dicer-CKO or control Dicer-fl/fl mice at indicated developmental stages were frozen sectioned, and immunostaining was performed using anti-phospho-Histone H3 (**A**, **B**) or anti-active Caspase3 (**C**, **D**) antibodies. Nuclei were visualized by staining with DAPI. (**A**–**D**) E17 to P1. *Lower* panels are enlarged images of the *white squared regions* in the *upper* panels. *Lower right* panels are without DAPI signals. (**A**, **B**) P5. *Upper* panels show peripheral retinas, and *lower* panels show central retinas. (**C**, **D**) P5. Images of the central region of retinas are shown. *Right* panels are without DAPI. (**E**, **F**) Phospho-Histone 3–positive cells in the central region of retina (100-μm wide) were counted at each stage, and the cell number (**E**) and positive cell population in percentages (**F**) are shown. The average of three independent retinas with SD is shown. Scale bars are as indicated.

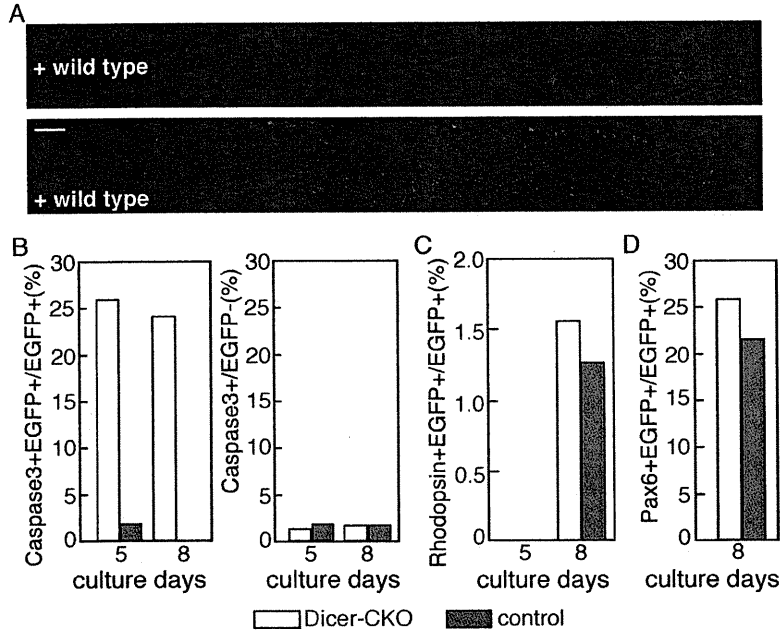

FIGURE 6. Cell death of retinal cells by deletion of Dicer occurred cell autonomously. Re-aggregation culture of retinal cells from Dicer-CKO/GFP or control was performed. Retinal cells at E16.5 were dissociated, mixed with excessively large numbers of host normal cells, and cultured for 12 days. Then re-aggregation cultures were harvested, frozen sectioned, and examined for proliferation and differentiation by immunostaining. (**A**) Sections were immunostained with anti-GFP antibody, and nuclei were visualized by staining of DAPI. Scale bar, 100 μm. (**B–D**) Apoptotic cells (**B**), rhodopsin (**C**)-, and Pax6 (**D**)-positive cells were examined by immunostaining using anti active-caspase3, rhodopsin, and Pax6 antibody, respectively. Double staining with GFP antibody was performed, and marker and EGFP double-positive populations (%) in total EGFP-positive cells are shown. (**B**, *right*) Caspase 3-positive cells in the EGFP-negative population. The same set of experiments was conducted three times, and essentially the same results were obtained.

induction of Cre expression in some retinal progenitor cells might have resulted in their survival, allowing them to differentiate. In the experiments involving Cre expression at the P1 stage, we found a lack of expression of PKC, which is a marker for bipolar cells, and a lower level of Islet1, which is a marker of ganglion and amacrine cells. Taking all our results together, the effects of the deletion of Dicer in retinal progenitor cells might not have been simply a shift of competency of retinal progenitor cells to retinal cells born early. The explanation may be more complex and may depend on the stage of retinal cells. However, given that the lamination of retinal cells had not been observed in any of the differentiation markers, we cannot use information about the subretinal localization of cells to determine whether the expression marker represented fully differentiated retinal cells.

In fact, we observed that the Dicer-CKO retina failed to form laminated retinal structures, and it is difficult to identify which marker-positive cells are equivalent to those in control retinas. Georgi and Reh[18] reported that the formation of GCL and INL was absent. However, Sox2 and Pax6—both retinal progenitor markers—showed relatively normal lamination in the embryonic retina of Dicer-CKO. We observed—at least from E16—no segregation of postmitotic cells or proliferating cells in the Dicer-CKO retina. Among all examinations of immunostaining, only normal positioning of cells was observed in those cells at the M phase that were marked by anti-phospho-Histone H3 antibody. In addition, we observed no layer structure in Dicer mice. In Dicer-CKO mice, the IPL was not clearly observed, suggesting that miRNA regulates the formation process of retinal cells. This suggests that Dicer is less critical for determining the fate of the retina but is critical for the migration and maturation of retinal cells. Taken together, these results show that Dicer is essential to retinal progenitor cell proliferation and survival in the retina during its early development, as in other organs. In addition, even after differentiation, Dicer is essential to cell survival and the final differentiation of retinal cells.

The initial report of retina-specific inactivation of Dicer by Chx10-Cre showed that morphologic defects at P16 progressed to more general cellular disorganization and widespread degeneration of retinal cell types as the animals aged.[17] In this study, the authors stated that the crucial role of Dicer is long-term regulation or retinal cell lamination, survival, and function, with no visible impact on early postnatal retinal structure or function. In our Dicer-CKO mice, at P16, we could not detect any retina-like structure; although some cells remained around the lens, these cells were active caspase3-positive. In contrast, Georgi and Reh[18] and we observed massive cell death at an early stage of retinal development. Because the same Dicer-flox mice[14] were used in the studies, this might have been due to differences in the Cre mice. Damiani et al.[28] used Chx10-Cre mice, made by using a *Chx10*-BAC construct. Chx10-BAC reporter analysis showed that the *Chx10* enhancer drives downstream genes beginning from at least E11.5. However, mosaic expression of target genes in the retina was observed.[28] Mosaic expression of Cre was also observed in Chx10-Cre/Dicer-flox mice.[17] Based on the lack of a severe phenotype, it was surmised that either miRNAs in the retina are extremely stable or that an additional protein can compensate for Dicer function during early postnatal life.[17] Georgi and Reh[18] discussed the possibility of non–cell-autonomous rescue of the phenotype of the Chx10-Cre/Dicer-deficient retina and

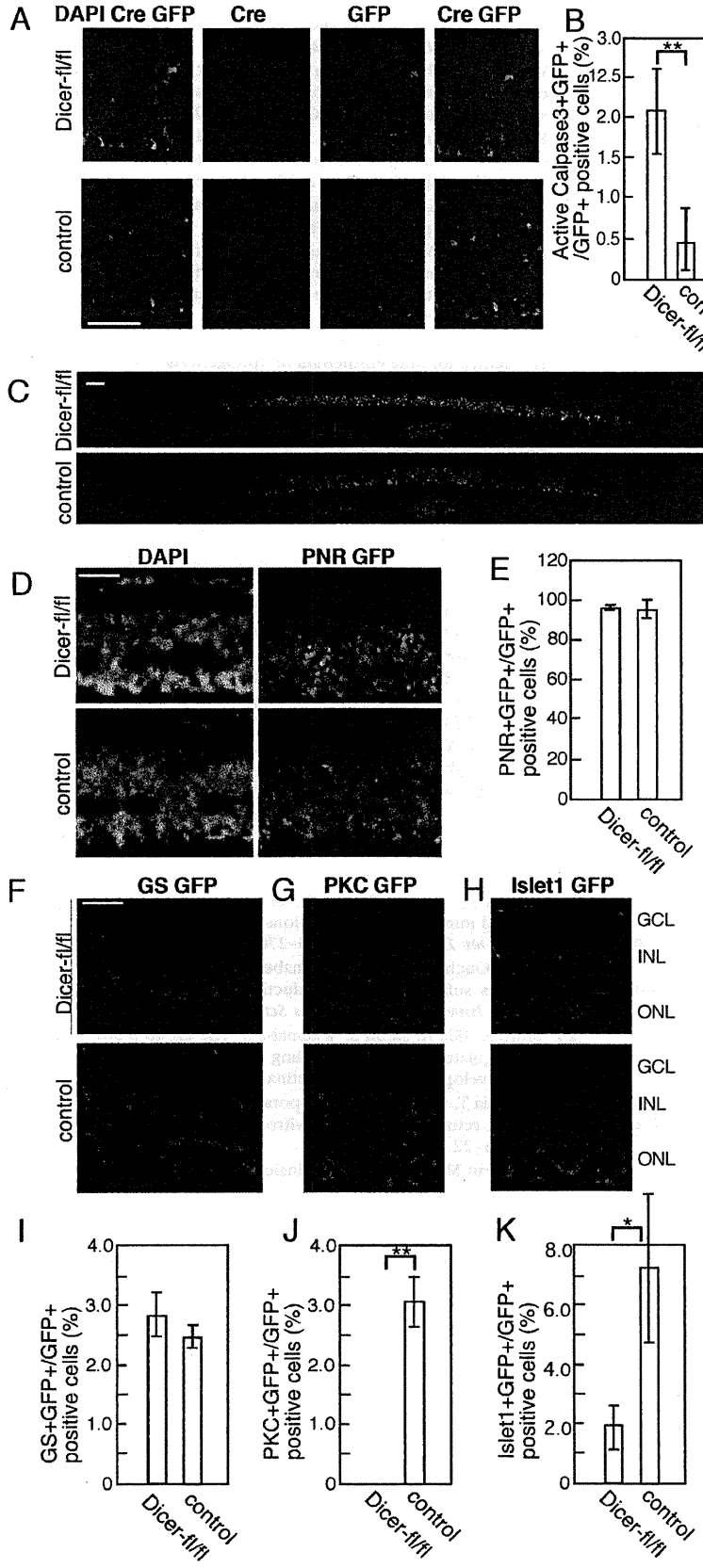

FIGURE 7. Expression of Cre at P1 Dicer-CKO retina resulted in enhanced apoptosis and perturbation of differentiation. (A) pCAG-Cre-IRES-EGFP was introduced into the retina at P1 of wild-type mice by electroporation. After 12 days of culture, expression of Cre and EGFP was examined by anti-Cre and -EGFP antibodies, respectively, by immunostaining of frozen sections. Similar results were obtained when we used retinas from Dicer-fl/fl mice. Scale bar, 50 μm. (B–G) pCAG-Cre-IRES-EGFP was introduced into retinas at P1 of control (wild-type) or Dicer-CKO and was cultured for 12 days. Apoptosis was examined by anti-active Caspase 3 antibody, and positive cells in the central retinal region (100 μm wide) were counted semiquantitatively in EGFP-positive cells (B). Differentiation of cells into photoreceptor (C–E), Müller glia (F, I), bipolar (G, J), or ganglion/amacrine (H, K) was examined by immunostaining with anti-PNR, GS, PKC, or Islet1 antibodies, respectively. Populations of PNR (E)-, GS (I)-, PKC (J)-, or Islet1 (K)-positive cells in total EGFP-positive cells were calculated semiquantitatively in the central retinal region (100 μm wide). The average of three independent retinas with SD is shown. $^{**}P < 0.01$ and $^{*}P < 0.05$ were calculated by Student's t-test. Nuclei were visualized by staining of DAPI. Scale bars: 100 μm (B), 50 μm (C), 100 μm (E), and 50 (F) μm.

the difference of onset of Cre in these mice. However, our observation of reaggregation culture suggested that the effects of deletion of Dicer are cell autonomous. The electroporation of Cre-expressing plasmid suggested that the severe effects of Cre deletion may be unrelated to the timing of expression, at least until the neonatal stage. Therefore, we postulated that mosaic expression of Cre is a less likely explanation of the phenotype. Furthermore, it seems unlikely that stable miRNA and other Dicer-like proteins are present in Chx10-Cre/Dicer-deficient retina. One possible reason is that the numbers of retinal progenitor cells expressing Cre may be too small in Chx10-Cre/Dicer-flox mice during early developmental stages and that the elimination of these cells was negligible in comparison with healthy cells or did not affect the gross morphology of the retina during development. Consequently, Chx10-Cre may turn on after birth in bipolar cells and cause the later phenotype.

The ubiquitous expression of Cre in retinal progenitor cells afforded by use of the Dkk3-promoter has enabled clarification of the essential role played by Dicer in retinal development.

Acknowledgments

The authors thank Takahisa Furukawa for providing Dkk3-Cre mice; Robert Whittier, Itsuki Ajioka, Shuji Takada, and Yoko Tabata for discussions and technical advice; Yumiko Ishii and the FACS core laboratory for technical support with sorting; and Dovie Wylie for excellent language assistance.

References

1. Marquardt T, Gruss P. Generating neuronal diversity in the retina: one for nearly all. *Trends Neurosci.* 2002;25:32-38.
2. Cepko CL. The roles of intrinsic and extrinsic cues and bHLH genes in the determination of retinal cell fates. *Curr Opin Neurobiol.* 1999;9:37-46.
3. Harris WA. Cellular diversification in vertebrate retina. *Curr Opin Genet Dev.* 1997;7:651-658.
4. Inui M, Martello G, Piccolo S. MicroRNA control of signal transduction. *Nat Rev Mol Cell Biol.* 2010;11:252-263.
5. Li X, Jin P. Roles of small regulatory RNAs in determining neuronal identity. *Nat Rev Neurosci.* 2010;11:329-338.
6. Mallanna SK, Rizzino A. Emerging roles of microRNAs in the control of embryonic stem cells and the generation of induced pluripotent stem cells. *Dev Biol.* 2010;344:16-25.
7. Decembrini S, Bressan D, Vignali R, et al. MicroRNAs couple cell fate and developmental timing in retina. *Proc Natl Acad Sci USA.* 2009;106:21179-21184.
8. Conte I, Carrella S, Avellino R, et al. miR-201 is required for lens and retinal development via Meis2 targeting. *Proc Natl Acad Sci USA.* 2010;107:15491-15496.
9. Krol J, Busskamp V, Markiewicz I, et al. Characterizing light-regulated retinal microRNAs reveals rapid turnover as a common property of neuronal microRNAs. *Cell.* 2010;141:618-631.
10. Gregory RI, Chendrimada TP, Schiekhattar R. MicroRNA biogenesis: isolation and characterization of the microprocessor complex. *Methods Mol Biol.* 2006;342:23-47.
11. Wang JY, Medvid R, Melton C, Jaenisch R, Blelloch R. DGCR8 is essential for microRNA biogenesis and silencing of embryonic stem cell self-renewal. *Nat Genet.* 2007;39:380-385.
12. Kanellopoulou C, Muljo SA, Kung AL, et al. Dicer-deficient mouse embryonic stem cells are defective in differentiation and centromeric silencing. *Gene Dev.* 2005;19:489-501.
13. Bernstein E, Kim D-KSY, Carmell MA, et al. Dicer is essential for mouse development. *Nat Genet.* 2003;35.
14. Harfe BD, McManus MT, Mansfield JH, Hornstein E, Tabin CJ. The RNaseII enzyme Dicer is required for morphogenesis but not patterning of the vertebrate limb. *Proc natl Acad Sci USA.* 2005;102:10898-10903.
15. Harris KS, Zhang Z, McManus MT, Harfe BD, Sun X. Dicer function is essential for lung epithelium morphogenesis. *Proc Natl Acad Sci USA.* 2006;2208-2213.
16. Davis TH, Cuellar TL, Koch SM, et al. Conditional loss of Dicer disrupts cellular and tissue morphogenesis in the cortex and hippocampus. *J Neurosci.* 2008;28:4322-4330.
17. Damiani D, Alexander JJ, O'Rourke JR, et al. Dicer inactivation leads to progressive functional and structural degeneration of the mouse retina. *J Neurosci.* 2008;28:4878-4887.
18. Georgi SA, Reh TA. Dicer is required for the transition from early to late progenitor state in the developing mouse retina. *J Neurosci.* 2010;30:4048-4061.
19. Sato S, Inoue T, Terada K, et al. Dkk3-cre bac transgenic mouse line: a tool for highly efficient gene deletion in retinal progenitor cells. *Genesis.* 2007;45:502-507.
20. Okabe M, Ikawa M, Kominami K, Nakanishi T, Nishimune Y. 'Green mice' as a source of ubiquitous green cells. *FEBS Lett.* 1997;407:313-319.
21. Ikawa M, Yamada S, Nakanishi T, Okabe M. Green fluorescent protein (GFP) as a vital marker in mammals. *Curr Top Dev Biol.* 1999;44:1-20.
22. Tabata Y, Ouchi Y, Kamiya H, Manabe T, Arai K, Watanabe S. Retinal fate specification of mouse embryonic stem cells by ectopic expression of Rx/rax, a homeobox gene. *Mol Cell Biol.* 2004;24:4513-4521.
23. Koso H, Ouchi Y, Tabata Y, et al. SSEA-1 marks regionally restricted immature subpopulations of embryonic retinal progenitor cells. *Dev Biol.* 2006;292:265-276.
24. Lin Y, Ouchi Y, Satoh S, Watanabe S. The HMG-transcription factor Sox2 is sufficient for the induction of amacrine cells in mouse retina. *Invest Ophthalmol Vis Sci.* 2008;50:68-74.
25. Muto A, Iida A, Satoh S, Watanabe S. The group E Sox8 and Sox9 are regulated by Notch signaling and are required for Muller glial cell development in mouse retina. *Exp Eye Res.* 2009;89:549-558.
26. Matsuda T, Cepko CL. Electroporation and RNA interference in the rodent retina in vivo and in vitro. *Proc Natl Acad Sci USA.* 2004;101:16-22.
27. Belliveau MJ, Cepko CL. Extrinsic and intrinsic factors control the genesis of amacrine and cone cells in the rat retina. *Development.* 1999;126:555-566.
28. Rowan S, Cepko CL. Genetic analysis of the homeodomain transcription factor Chx10 in the retina using a novel multifunctional BAC transgenic mouse reporter. *Dev Biol.* 2004;271:388-402.

Int J Hematol (2011) 94:81–89
DOI 10.1007/s12185-011-0883-y

ORIGINAL ARTICLE

Expression of myeloperoxidase and gene mutations in AML patients with normal karyotype: double *CEBPA* mutations are associated with high percentage of MPO positivity in leukemic blasts

Shinya Tominaga-Sato · Hideki Tsushima · Koji Ando · Hidehiro Itonaga · Yoshitaka Imaizumi · Daisuke Imanishi · Masako Iwanaga · Jun Taguchi · Takuya Fukushima · Shinichiro Yoshida · Tomoko Hata · Yukiyoshi Moriuchi · Kazutaka Kuriyama · Hiroyuki Mano · Masao Tomonaga · Yasushi Miyazaki

Received: 22 March 2011 / Revised: 23 May 2011 / Accepted: 23 May 2011 / Published online: 16 June 2011

Abstract The percentage of myeloperoxidase (MPO)-positive blast cells is a simple and highly significant prognostic factor in AML patients. It has been reported that the high MPO group (MPO-H), in which >50% of blasts are MPO activity positive, is associated with favorable karyotypes, while the low MPO group (≤50% of blasts are MPO activity positive, MPO-L) is associated with adverse karyotypes. The MPO-H group shows better survival even when restricted to patients belonging to the intermediate chromosomal risk group or those with a normal karyotype. It has recently been shown that genotypes defined by the mutational status of *NPM1*, *FLT3*, and *CEBPA* are associated with treatment outcome in patients with cytogenetically normal AML. In this study, we aimed to evaluate the relationship between MPO positivity and gene mutations found in normal karyotypes. Sixty AML patients with normal karyotypes were included in this study. Blast cell MPO positivity was assessed in bone marrow smears stained for MPO. Associated genetic lesions (the *NPM1*, *FLT3*-ITD, and *CEBPA* mutations) were studied using nucleotide sequencing. Thirty-two patients were in the MPO-L group, and 28 patients in the MPO-H group. *FLT3*-ITD was found in 11 patients (18.3%), *NPM1* mutations were found in 19 patients (31.7%), and *CEBPA* mutations were found in 11 patients (18.3%). In patients with *CEBPA* mutations, the carrying two simultaneous mutations ($CEBPA^{double\text{-}mut}$) was associated with high MPO expression, while the mutant *NPM1* without *FLT3*-ITD genotype was not associated with MPO activity. Both higher MPO expression and the $CEBPA^{double\text{-}mut}$ genotype appeared to be associated with improved overall survival after intensive chemotherapy. Further studies are required to determine the importance of blast MPO activity as a prognostic factor, especially in *CEBPA* wild-type patients with a normal karyotype.

S. Tominaga-Sato · H. Itonaga · M. Iwanaga · J. Taguchi · Y. Miyazaki
Department of Hematology and Molecular Medicine Unit, Atomic Bomb Disease Institute, Nagasaki University Graduate School of Biomedical Sciences, Nagasaki, Nagasaki, Japan

H. Tsushima (✉) · Y. Imaizumi · D. Imanishi · T. Fukushima · T. Hata
Department of Hematology, Nagasaki University Hospital, 1-7-1 Sakamoto, Nagasaki 852-8501, Japan
e-mail: tsushima@nagasaki-u.ac.jp

K. Ando · S. Yoshida
Department of Internal Medicine, Nagasaki National Medical Center, Ohmura, Nagasaki, Japan

Y. Moriuchi
Division of Hematology, Sasebo City General Hospital, Sasebo, Nagasaki, Japan

K. Kuriyama
School of Health Sciences, University of the Ryukyus, Okinawa, Nishihara, Japan

H. Mano
Division of Functional Genomics, Jichi Medical University, Shimotsuke, Tochigi, Japan

M. Tomonaga
Department of Hematology, Japanese Red-Cross Nagasaki Atomic Bomb Hospital, Nagasaki, Nagasaki, Japan

Keywords Acute myeloid leukemia · Normal karyotype · Myeloperoxidase · *CEBPA* mutations

1 Introduction

The AML87, -89, and -92 studies conducted by Japan Adult Leukemia Study Group (JALSG) revealed that patient age, ECOG performance status, leukocyte count, FAB subclass, the number of induction courses required to achieve complete remission (CR), the presence of good prognostic chromosomal abnormalities [t(8;21) or inv(16)], and percentage of myeloperoxidase (MPO)-stained positive blast cells at diagnosis were significant risk factors for overall survival (OS) of patients with acute myeloid leukemia (AML) [1]. In more recent AML201 study, it was shown that significant unfavorable prognostic features for OS were adverse cytogenetic risk group [2], age of more than 50 years, WBC more than 20×10^9/L, FAB classification of either M0, M6, or M7, and MPO-positive blasts less than 50% [3]. These observations imply that the percentage of MPO-positive blast cells is one of the important prognostic markers along with cytogenetics and molecular genetic information.

MPO, a microbicidal protein, is considered to be a golden marker for the diagnosis of AML in the French–American–British (FAB) and WHO classifications [4, 5]. In our previous reports [6–8], AML patients with a high percentage of MPO-positive blasts (>50% of blasts are MPO activity positive, MPO-H) had a significantly better complete remission (CR) rate, disease-free survival, and overall survival compared with the low MPO activity positive blast group (≤50% of blasts are MPO activity positive, MPO-L). Most patients with a favorable chromosomal risk profile were in the MPO-H group, and most of the patients with an adverse chromosomal risk profile were in the MPO-L group. The difference in OS between the low and high MPO groups was still observed in a cohort of patients with normal karyotypes, suggesting that MPO is highly expressed in the leukemic blasts of AML patients with a favorable prognosis. To fully understand this phenomenon, it would be important to analyze genetic factors associated with MPO expression, especially in patients with a normal karyotype.

In the WHO classification, mutations of *FLT3*, *NPM1* and *CEBPA* have been emphasized to have prognostic significance in AML patients with normal karyotype. The nucleophosmin 1 gene (*NPM1*) has been shown to be mutated in 45–64% of AML cases with a normal karyotype [9, 10], and *NPM1* mutations are associated with a favorable prognosis in the absence of the internal tandem duplication (ITD) type of fms-related tyrosine kinase-3 gene (*FLT3*) mutation, a known adverse prognostic factor [11]. The CCAAT/enhancer binding protein-alpha gene (*CEBPA*) is another gene that has been shown to be mutated in AML patients with a normal karyotype [12, 13]. Mutations in the *CEBPA* gene are found in 5–14% of all AML cases and are associated with a relatively favorable outcome, and hence, have gained interest as a prognostic marker [14]. Recently, it has been shown that most AML patients with *CEBPA* mutations carry 2 simultaneous mutations ($CEBPA^{\text{double-mut}}$), whereas single mutations ($CEBPA^{\text{single-mut}}$) are less common. In addition it was found that the $CEBPA^{\text{double-mut}}$ genotype is associated with a favorable overall and event-free survival [15, 16]. It is still unclear why $CEBPA^{\text{double-mut}}$ AML patients have better outcomes than those with a single heterozygous mutation.

In this study, we retrospectively examined 60 de novo adult AML patients with normal karyotypes in order to obtain a better insight into the relationships between MPO positivity and other prognostic factors (*NPM1*, *FLT3*, and *CEBPA* mutations). In line with previous reports, both high MPO positivity in AML blasts and the $CEBPA^{\text{double-mut}}$ genotype appeared to be associated with a favorable outcome, and it appeared that it was the $CEBPA^{\text{double-mut}}$ genotype that associated with high blast MPO activity.

2 Materials and methods

2.1 Patients and treatments

The study population included 60 patients with newly diagnosed de novo AML that had been treated at the Department of Internal Medicine, Nagasaki National Medical Center, between 1990 and 2010. All patients had normal karyotype AML. AML was diagnosed according to the FAB classification. Two members independently assessed the percentage of MPO-positive blast cells in MPO-stained bone marrow smears. The main biological and clinical features of the patients are shown in Table 1. Excluding the 25 patients who did not receive conventional induction chemotherapy, all patients were treated according to the Japan Adult Leukemia Study Group (JALSG) protocols (AML89, -92, -95, -97, and -201 studies) [3, 17–19]. CR was determined as when blasts accounted for less than 5% of the cells in normocellular bone marrow with normal peripheral neutrophil and platelet counts. This study was approved by the Ethical Committees of the participating hospitals.

2.2 Analysis of the *FLT3*, *NPM1*, and *CEBPA* genes

High molecular weight genomic DNA was extracted from bone marrow and peripheral blood samples after Ficoll

Table 1 Characteristics of de novo AML patients with a normal karyotype

	All patients ($n = 60$)	Patients who received intensive chemotherapy ($n = 36$)
Median age (range) (year)	59.5 (15–81)	49 (15–67)
Male/female	32/28	18/18
FAB type		
M0	5	3
M1	10	5
M2	21	14
M4	18	11
M5	3	1
M6	3	2
M7	0	0
WBC ($\times 10^9$/L), median (range)	14.9 (0.7–556)	13.0 (0.7–246)
Performance status		
0–2	55	34
3–4	5	2
LDH (IU/L), median (range)	296 (120–5,325)	291 (140–2,606)
MPO		
Low (≤50%)	32	20
High (>50%)	28	16

FAB French–American–British, *WBC* white blood cells, *LDH* lactate dehydrogenase, *MPO* myeloperoxidase

separation of mononucleated cells (35 and 4 patients, respectively) using the QIAamp DNA Mini Kit (Qiagen, Hilden, Germany). In addition, we isolated genomic DNA from the BM smears of the AML patients (21 samples) using the QIAamp DNA blood Mini Kit (Qiagen, Hilden, Germany).

Mutations in the *FLT3*, *NPM1*, and *CEBPA* genes were detected by genomic DNA PCR and direct sequencing. Exons 14 and 15 and the intervening intron of the *FLT3* gene were amplified from DNA using the previously described primers FLT3-11F and FLT3-12R [20]. PCR for NPM1 exon 12 was performed with genomic DNA, the same reagent, and the published primer molecules NPM1-F and NPM1-R [21]. PCR for *CEBPA* was performed using 2 overlapping primer pairs: CEBPA-CT3F (5′-TGCCGGGTATAAAA-GCT GGG-3′) and CT3R (5′-CTCGTTGCTGTTCTTGTCCA -3′), CEBPA-PP2F (5′-TGCCGGGT-ATAAAAGCTGG G-3′) and PP2R (5′-CACGGTCTGGGCAAGCCTCG AGAT-3′). The PCR reactions were run in a final volume of 50 μL containing 10 ng DNA, 5× buffer, 0.2 mmol/L of each deoxynucleotide triphosphate, primers (0.3 μmol/L of each), nucleotides (0.2 mmol/L of each), and 1 U of KOD-Plus-Neo polymerase (TOYOBO, Osaka, Japan). The mixture was initially heated at 94°C for 2 min, before being subjected to 35 cycles of denaturation at 94°C for 10 s and annealing and extension at 68°C for 1 min. The amplified products were cut out from a 1.2% agarose gel and purified with the MinElute Gel extraction kit (QIAGEN, Germany). To screen for mutations, the PCR products were sequenced in both directions with the following primers: FLT3-11F, FLT3-12R, NPM1-F, NPM-R, CEBPA-CT1F, CEBPA-1R, CEBPA-PP2F, CEBPA-PP2R, CEBPA-2F (5′-GCTG GGCGGCATCTGCG-A-3′), and CEBPA-1R (5′-TGT-GC TGGAACAGGTCGGCCA-3′) using a BigDye Terminator v3.1 Cycle Sequencing Kit and the ABI Prism 3100 ×1 Genetic Analyzer (Applied Biosystems, CA, USA). In the case of *NPM1* and *CEBPA* genes, when heterozygous data were identified by sequence screening, mutations were confirmed by cloning with the StrataClone Blunt PCR Cloning Kit (Stratagene, CA, USA) according to the manufacturer's recommendations. Four to ten recombinant colonies were chosen and cultured in LB medium. Plasmid DNA was prepared using a QIAprep spin plasmid miniprep kit (Qiagen, Hilden, Germany), and both strands were sequenced using the T3 and T7 primers and the CEBPA-2F and CEBPA-1R primers.

2.3 Statistical methods

To evaluate the relationship between the frequency of mutations status and clinical characteristics, the following variables were included in the analysis: age, FAB classification, peripheral WBC count, MPO-positivity rate, JALSG score [1], and CR achievement. A comparison of frequencies was performed using Fisher's exact test. Differences in percentage of MPO-positive blasts among patients with different mutational status of genes were compared using the non-parametric Kruskal–Wallis test and followed by Dunn's multiple comparison post-test. Overall survival (OS) was calculated using the Kaplan–Meier method [22], and the group differences were compared using the log-rank test. Thirteen patients who underwent allogeneic or autologous hematopoietic stem cell transplantation were not censored at the time of transplantation. For all analyses, statistical significance was considered at the level of two-tailed 0.05.

3 Results

3.1 Patients' characteristics

As shown in Table 1, the series included 60 patients. Their median age was 59.5 (15–81 years), and there were 32 males (53.3%) and 28 females (46.7%). All patients had normal cytogenetics. Using the percentage of MPO-positive leukemic blasts, as judged from bone marrow slides, the cases

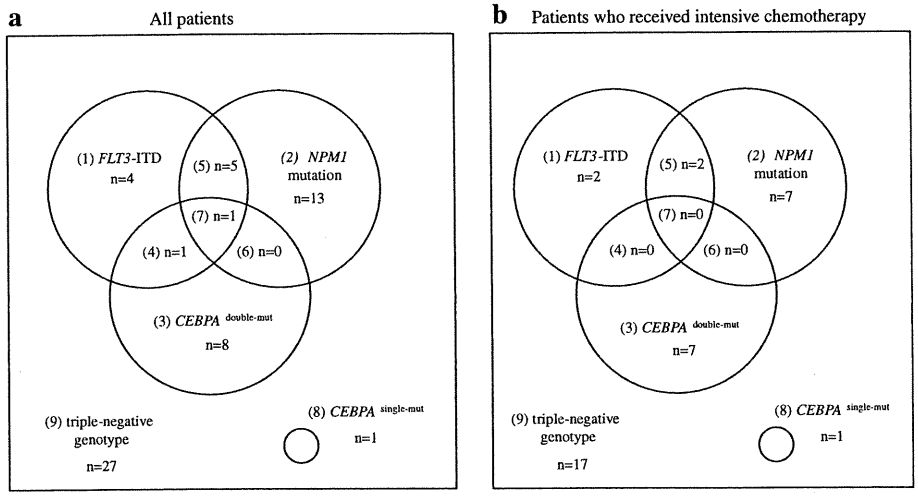

Fig. 1 Frequency and overlapping patterns of AML patients with a normal karyotype. Data are shown for all patients (**a**) and for patients who received intensive chemotherapy (**b**). **a** (*1*) *FLT3*-ITD + wt *NPM1* + wt *CEBPA* ($n = 4$, 6.7%), (*2*) wt *FLT3* + *NPM1* mutation + wt *CEBPA* ($n = 13$, 21.7%), (*3*) wt *FLT3* + wt *NPM1* + $CEBPA^{double\text{-}mut}$ ($n = 8$, 13.3%), (*4*) *FLT3*-ITD + wt *NPM1* + $CEBPA^{double\text{-}mut}$ ($n = 1$, 1.7%), (*5*) *FLT3*-ITD + *NPM1* mutation + wt *CEBPA* ($n = 5$, 8.3%), (*6*) wt *FLT3* + *NPM1* mutation + $CEBPA^{double\text{-}mut}$ ($n = 0$, 0%), (*7*) *FLT3*-ITD + *NPM1* mutation + $CEBPA^{double\text{-}mut}$ ($n = 1$, 1.7%), (*8*) wt *FLT3* + wt *NPM1* + $CEBPA^{single\text{-}mut}$ ($n = 1$, 1.7%), (*9*) triple-negative genotype ($n = 27$, 45%). **b** (*1*) *FLT3*-ITD + wt *NPM1* + wt *CEBPA* ($n = 2$, 5.6%), (*2*) wt *FLT3* + *NPM1* mutation + wt *CEBPA* ($n = 7$, 19.4%), (*3*) wt *FLT3* + wt *NPM1* + $CEBPA^{double\text{-}mut}$ ($n = 7$, 19.4%), (*4*) *FLT3*-ITD + wt *NPM1* + $CEBPA^{double\text{-}mut}$ ($n = 0$, 0%), (*5*) *FLT3*-ITD + *NPM1* mutation + wt *CEBPA* ($n = 2$, 5.6%), (*6*) wt *FLT3* + *NPM1* mutation + $CEBPA^{double\text{-}mut}$ ($n = 0$, 0%), (*7*) *FLT3*-ITD + *NPM1* mutation + $CEBPA^{double\text{-}mut}$ ($n = 0$, 0%), (*8*) wt *FLT3* + wt *NPM1* + $CEBPA^{single\text{-}mut}$ ($n = 0$, 0%), (*9*) triple-negative genotype ($n = 17$, 47.2%). *wt* wild-type

were divided into the High group (MPO-positive blasts > 50%) and Low group (MPO-positive blasts ≤ 50%). Thirty-two patients were classified into the Low group, and 28 patients were classified into the High group.

3.2 Mutational analysis

FLT3-ITD was found in 11 patients (18.3%), *NPM1* mutations were found in 19 patients (31.7%), and *CEBPA* mutations were found in 11 patients (18.3%). Frequency and an overlapping pattern of mutations are shown in Fig. 1. Among the patients with *CEBPA* mutations, approximately 90% (10 of 11 patients) of the patients had two *CEBPA* mutations ($CEBPA^{double\text{-}mut}$), whereas 10% (1 of 11 patients) had a single mutation. As previously reported, the mutations in the $CEBPA^{double\text{-}mut}$ patients were clustered in the N- and C-terminal hotspots (Table 2; Fig. 2). *FLT3*-ITD mutation was associated with a higher WBC at the time of diagnosis, as reported previously. Neither *NPM1* nor *CEBPA* mutation status displayed a significant association with age, PS, WBC, FAB subtype, JALSG score, or CR achievement (Table 3).

3.3 Clinical outcome

OS was analyzed only in patients who received intensive chemotherapy ($n = 36$). They received chemotherapy based on the treatment protocol described in the JALSG AML89, -92, -95, -97, and -201 studies. As reported previously [6], we observed an association between the percentage of MPO-positive blasts and the survival rate in the normal karyotype patients treated with intensive chemotherapy, although the significance in this cohort was rather low ($P = 0.10$) (Fig. 3). Figure 4 shows Kaplan–Meier curves according to genotype. 'Other genotypes' included the *FLT3*-ITD genotype, the $CEBPA^{single\text{-}mut}$ genotype, and the triple-negative genotype consisting of the wild-type *NPM1* and *CEBPA* genotypes without *FLT3*-ITD. In line with previous reports [14], the patients with the $CEBPA^{double\text{-}mut}$ genotype tended to show higher survival rate compared with patients displaying other genotypes ($P = 0.07$). In this study, the mutant *NPM1* without *FLT3*-ITD genotype was not significantly associated with treatment outcome, possibly due to the small number of patients.

3.4 Difference of MPO-positivity rate by gene mutation status

Figure 5 shows the level of the percentage of MPO-positive blasts by gene mutational status of the *CEBPA*, *FLT3*-ITD, and *NPM1*. The MPO-positivity rate was very high, over 50% (median 96, range 71–100), in all $CEBPA^{double\text{-}mut}$ cases, but it was 20% in one case displaying the

Table 2 Genetic findings of the patients with *CEBPA* mutations

Patient	Category	Nucleotide changes	Amino acid changes	Comments
4	Double	218_219insC	P23fsX107	Produces N-terminal stop codon
		1129_1130insATGTGGAGACGCAGCAGAAGGTGCTGGAGCTG ACCAGTGACAATGACCGCCTGCGCAAGC	K326_327insHVETQQKVLELTSDNDRLRKR	In-frame insertion in bZIP
6	Double	200_218delinsCT	S16fsX101	Produces N-terminal stop codon
		1087_1089dup	K313dup	In-frame duplication in bZIP
7	Double	368_369insA	A72fsX107	Produces N-terminal stop codon
		1080_1082del	T310_Q311del	In-frame deletion in bZIP
13	Double	303_316del	P50fsX102	Produces N-terminal stop codon
		1062_1063insTTG	K304_Q305insV	In-frame insertion in bZIP
19	Double	215_225del	P21fsX103	Produces N-terminal stop codon
		1101_1102insCAGCGCAACGTGGAGACGCAGCAGA AGGTGCTGGAGCTG	L317_T318insQRNVETQQKVLEL	In-frame insertion in bZIP
22	Double	213del	P22fsX159	Produces N-terminal stop codon
		1064_1129dup	K304_Q305insQRNVETQQKVLELTSDNDRLRKR	In-frame insertion in bZIP
27	Double	324_328dup	E59fsX161	Produces N-terminal stop codon
		1062_1063insTTG	K304_Q305insV	In-frame insertion in bZIP
39	Double	213del	P22fsX159	Produces N-terminal stop codon
		1081_1086dup	Q311_Q312dup	In-frame duplication in bZIP
47	Double	397del	F82fsX159	Produces N-terminal stop codon
		1101_1102insCAGCGCAACGTGGAGACGCAGCA GAAGGTGCTGGAGCTG	L317_T318insQRNVETQQKVLEL	In-frame insertion in bZIP
49	Double	297_304del	A48fsX104	Produces N-terminal stop codon
		758del	A202fsX317	Frameshift between TAD2 and bZIP; produces stop codon in bZIP
35	Single	1087_1089dup	K313dup	In-frame duplication in bZIP

Nucleotide numbering was performed according to NCBI Entrez accession no. XM_009180.3, in which the major translational start codon starts at nucleotide position 151. The locations of functional domains are derived from Mueller and Pabst.1

bZIP basic leucine zipper region, *TAD2* second transactivation domain

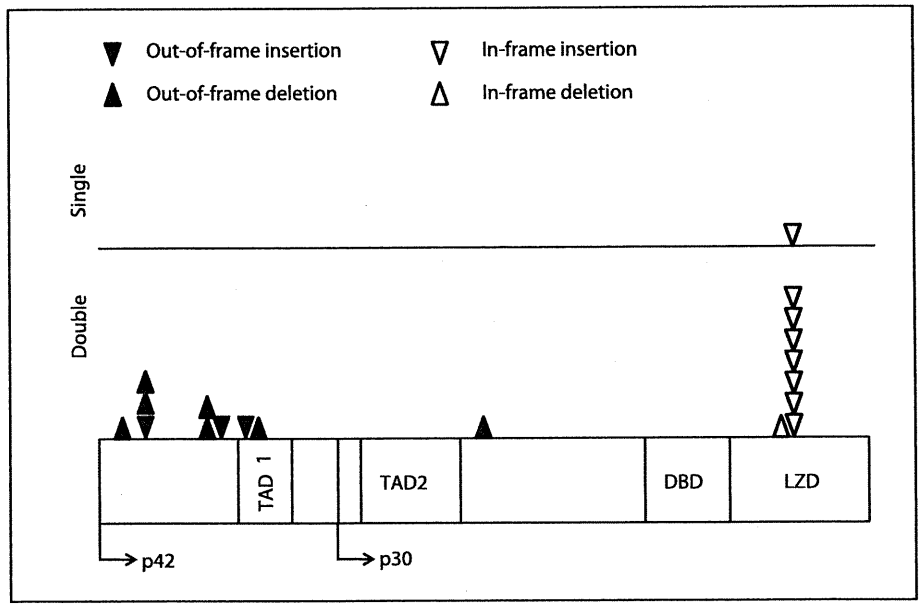

Fig. 2 Location of mutations detected in the *CEBPA*$^{single\text{-}mut}$ and *CEBPA*$^{double\text{-}mut}$ patients. Transactivation domain (TAD) 1, amino acids (AA) 70–97; p30 ATG, AA120; TAD2, AA 126–200; DNA-binding domain (DBD), AA 278–306; leucine zipper domain (LZD), AA 307–358

CEBPA$^{single\text{-}mut}$ genotype (data not shown). The MPO-positivity rate was widely distributed in patients who had mutant *NPM1* without *FLT3*-ITD genotype (median 26, range 0–100) and other genotypes (median 31, range 0–100). Kruskal–Wallis test showed that a significant difference of the MPO-positivity rate among three groups ($P = 0.005$). When comparing the individual groups by Dunn's Multiple Comparisons post hoc test for each group, there was a significant difference only for patients with *CEBPA*$^{double\text{-}mut}$ versus patients with other genotypes.

4 Discussion

While cytogenetic group is considered to be the primary prognostic indicator in AML, the percentage of MPO-positive blast cells could be used to predict the prognosis of patients with normal karyotypes [6]. In this study, we found that *CEBPA* gene mutational status has impact on the frequency of MPO expression: the patients with the *CEBPA* mutation genotype displayed a significantly higher percentage of cells expressing MPO than those with other genotypes ($P < 0.01$). The association was even more significant when analyzed without the *CEBPA*$^{single\text{-}mut}$ carrying patient, suggesting that high blast MPO activity is related to double *CEBPA* mutations. Although the mutant *NPM1* without *FLT3*-ITD genotype has been reported to be associated with a favorable prognosis in AML patients, there was no relationship between this type of mutation and the percentage of blasts showing MPO expression.

It is not clear how the *CEBPA*$^{double\text{-}mut}$ genotype enhances MPO activity in AML blasts. It has been shown that the MPO enhancer contains a *CEBPA* site contributing to its functional activity [23, 24], suggesting that the MPO gene is a major target of C/EBPα. Since it has been shown that both N-terminal frame-shift mutant and C-terminal mutant do not show transcriptional activity [25], we first speculated that mutations of the *CEBPA* gene might lead to decreased MPO activity, which turned out to be wrong. AML1 is another gene that has been reported to participate in up-regulation of MPO gene [26]. An AML1 site was identified in upstream enhancer of the human MPO gene, which appears to be necessary for maximal stimulation of MPO promoter activity. In patients with AML with t(8;21), the translocation results in an in-frame fusion between 5 exons of the AM1 gene and essentially all of the ETO gene producing a chimeric protein [27]. This protein, AML1-ETO, acts as a negative dominant inhibitor of wild-type AML1 [28], which theoretically could lead to down-regulation of AML1 target genes, such as MPO gene. However, blasts with t(8;21) have been shown to display higher levels of MPO expression both in clinical samples and in vitro experiments [29, 30], suggesting that the transcriptional alterations caused by these mutations are complex. The upregulation of blast MPO activity seen in CEBP/α$^{double\text{-}mut}$ cases may be due to alterations in the gene expression profile, rather than a simple dominant negative effect of mutated CEBP/α. Further experiments including investigation of transactivation potential of CEBP/α mutants on MPO promoter is necessary to clarify this mechanism.

CEBPA mutations are associated with a relatively favorable outcome, and it was recently shown in a multivariable analysis including cytogenetic risk and the

Table 3 Frequency *of FLT3*-ITD, *NPM1*, and *CEBPA* mutations by clinical characteristics in de novo AML cases with a normal karyotype

	FLT3		*P*	*NPM1*		*P*	*CEBPA*		*P*
	ITD ($n = 11$)	Other type ($n = 49$)		Mutation without *FLT3*-ITD ($n = 13$)	Other type ($n = 47$)		Double mutation without *FLT3*-ITD ($n = 8$)	Other type ($n = 52$)	
Age			0.08			0.74			0.10
≤50	1	19		5	15		5	15	
>50	10	30		8	32		3	37	
PS			1.00			0.20			0.52
0–2	10	45		11	45		7	48	
3–4	1	4		2	2		1	4	
WBC			0.02			1.00			1.00
≤20,000	2	30		7	25		4	28	
>20,000	9	19		6	22		4	24	
FAB subtype			0.33			0.18			0.58
M1, M2, M4, M5	11	41		13	39		8	44	
M0, M6, M7	0	8		0	8		0	8	
JALSG score[a]			0.79			0.72			0.09
Favorable	0	5		0	5		2	3	
Intermediate	2	18		5	15		5	15	
Adverse	2	9		2	9		0	11	
CR[a]			1.00			0.56			0.56
Achievement	4	27		7	24		7	24	
Failure	0	5		0	5		0	5	

[a] Analysis was carried in 36 patients with intensive chemotherapy

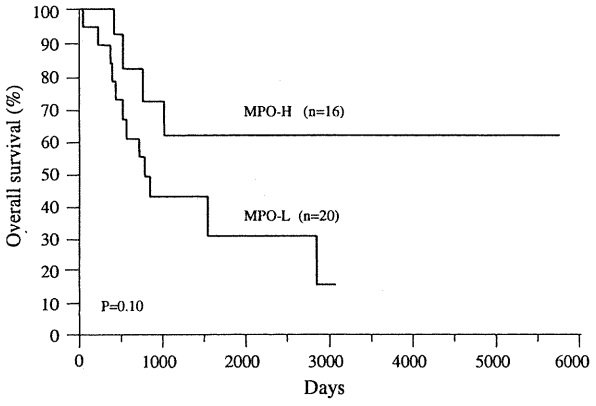

Fig. 3 Kaplan–Meier estimates of the probability of overall survival in 36 patients who received intensive chemotherapy, according to the percentage of myeloperoxidase-positive blasts. MPO-H (MPO-positive blasts: >50%) tended to have a positive effect on overall survival compared with MPO-L (MPO-positive blasts: ≤50%), although the difference was not statistically significant. The statistical significance of differences was evaluated with the log-rank test

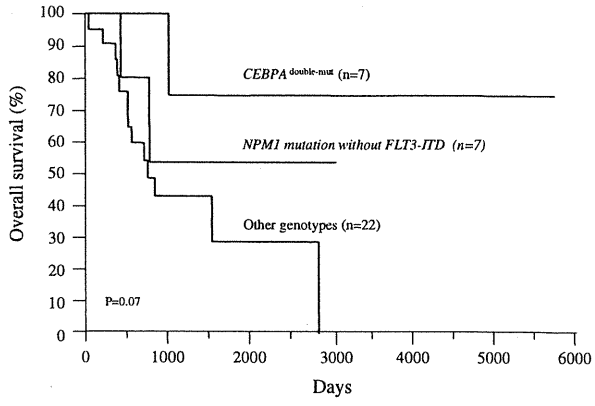

Fig. 4 Overall survival according to genotype in patients administered intensive chemotherapy. 'Other genotypes' was defined as the *FLT3*-ITD genotype, the *CEBPA*$^{\text{single-mut}}$ genotype, and the triple-negative genotype consisting of the wild-type *NPM1* and *CEBPA* genotypes without *FLT3*-ITD. The patients with the *CEBPA*$^{\text{double-mut}}$ genotype tended to show higher overall survival compared with the patients with 'other genotypes' ($P = 0.07$)

FLT3-ITD and *NPM1* mutations that the *CEBPA*$^{\text{double-mut}}$ genotype is associated with favorable overall and event-free survival [15, 16]. In a cohort of 60 cases of adult de novo AML, we identified 1 *CEBPA*$^{\text{single-mut}}$ case and 10 *CEBPA*$^{\text{double-mut}}$ cases, and in line with previous reports, our study tended to show better overall survival in *CEBPA*$^{\text{double-mut}}$ cases compared to cases with wild-type *CEBPA* in patients treated with intensive chemotherapy. We failed to find a prognostic effect in relation to the *CEBPA*$^{\text{double-mut}}$ in patients treated with low dose

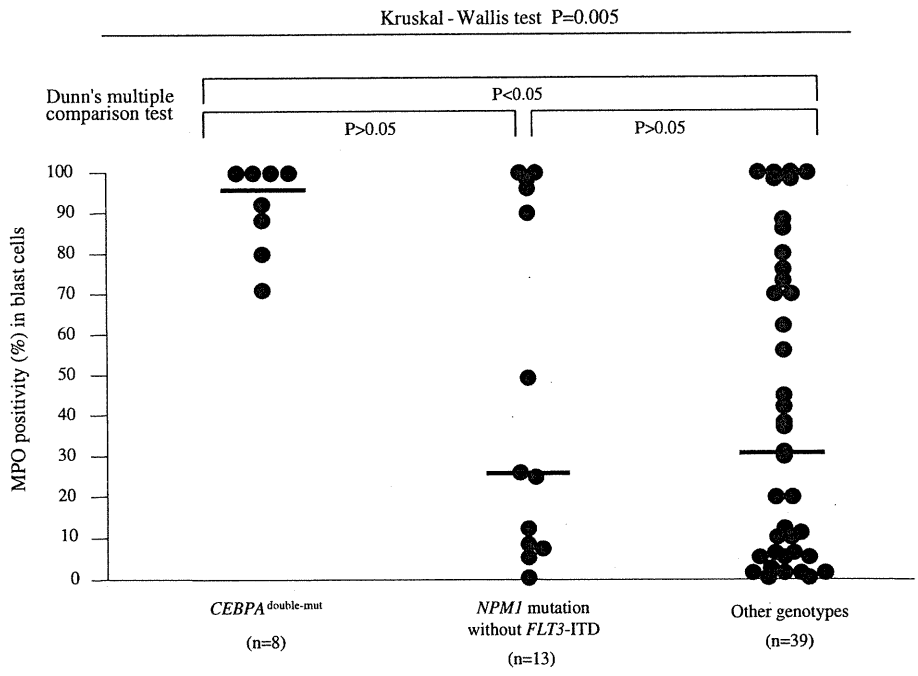

Fig. 5 MPO-positivity rate in blast according to genetic abnormalities in de novo AML patients with a normal karyotype. 'Other genotypes' was defined as the *FLT3*-ITD genotype, the *CEBPA*$^{single\text{-}mut}$ genotype, and the triple-negative genotype consisting of the wild-type *NPM1* and *CEBPA* genotypes without *FLT3*-ITD. The median MPO-positivity rate (*horizontal line*) was significantly different between the *CEBPA*$^{double\text{-}mut}$ genotype and 'other genotypes' (Kruskal–Wallis test followed by Dunn's multiple comparisons test: $P < 0.05$)

chemotherapy (data not shown), suggesting that the standard chemotherapy dose is necessary to improve the outcome of *CEBPA*$^{double\text{-}mut}$ cases.

It is unclear why *CEBPA*$^{double\text{-}mut}$ AML patients have a better outcome than those with *CEBPA* wild-type AML. One explanation is that high MPO expression leads to increased sensitivity to chemotherapeutic agents, such as to Ara-C [8]. To test this hypothesis, we also examined the association between blast MPO positivity and overall survival in *CEBPA* wild-type cases. Unexpectedly, when the patients were treated with intensive chemotherapy, the percentage of MPO-positive blasts was not significantly associated with overall survival in this group (data not shown), suggesting that the level of MPO expression itself is not responsible for the improvement in overall survival. However, as this analysis only involved 28 cases, we need to increase the number of cases in order to draw a definitive conclusion.

In summary, the data presented here suggested that the *CEBPA*$^{double\text{-}mut}$ genotype was associated with high MPO blast activity in patients with a normal karyotype. Although the results were obtained from a single institution, the presence of *CEBPA*$^{double\text{-}mut}$ genotype in high MPO group could explain, at least in part, why high MPO blast activity is associated with better overall survival. Further studies in a larger cohort of patients are necessary to assess blast MPO activity as a prognostic factor, especially in *CEBPA* wild-type patients with a normal karyotype.

Acknowledgments We would like to thank Dr. T Matsuo for his support, also Ms. N. Shirahama and Ms. M. Yamaguchi for their assistance. This work was supported in part by grant from the Ministry of Health, Labor and Welfare and Ministry of Education, Culture, Sports, Science and Technology of Japan.

Conflict of interest All authors have no conflict of interest to report.

References

1. Miyawaki S, Sakamaki H, Ohtake S, Emi N, Yagasaki F, Mitani K, et al. A randomized, postremission comparison of four courses of standard-dose consolidation therapy without maintenance therapy versus three courses of standard-dose consolidation with maintenance therapy in adults with acute myeloid leukemia. Cancer. 2005;104:2726–34.
2. David G, Helen W, Fiona O, Keith W, Christine H, Georgina H, et al. The importance of diagnostic cytogenetics on outcome in AML: analysis of 1, 612 patients entered into the MRC AML 10 trial. Blood. 1998;92:2322–33.
3. Ohtake S, Miyawaki S, Fujita H, Kiyoi H, Shinagawa K, Usui N, et al. Randomized study of induction therapy comparing standard-dose idarubicin with high-dose daunorubicin in adult patients with previously untreated acute myeloid leukemia: JALSG AML201 Study. Blood. 2011;117:2358–65.
4. Bennett JM, Catovsky D, Daniel MT, Flandrin G, Galton DA, Gralnick HR, et al. Proposed revised criteria for the classification of acute myeloid leukemia. A report of the French–American–British Cooperative Group. Ann Intern Med. 1985;103:620–5.
5. World Health Organization. Classification of tumors. In: Jaffe ES, Harris NL, Stein H, Vardimann JW, editors. Pathology and genetics of tumors of haematopoietic and lymphoid tissues. Lyon: IARC Press; 2001. p. 79–80.
6. Matsuo T, Kuriyama K, Miyazaki Y, Yoshida S, Tomonaga M, Emi N, et al. The percentage of myeloperoxidase-positive blast